Abrasion Resistance Evaluation Method For High-Density Polyethylene Jackets Used on Small Diameter Submarine Cables

by Kevin G. Booth

Applied Physics Laboratory   University of Washington
1013 NE 40th Street   Seattle, Washington 98105-6698

	Form Approved
# Report Documentation Page	*Form Approved* *OMB No. 0704-0188*

Public reporting burden for the collection of information is estimated to average 1 hour per response, including the time for reviewing instructions, searching existing data sources, gathering and maintaining the data needed, and completing and reviewing the collection of information. Send comments regarding this burden estimate or any other aspect of this collection of information, including suggestions for reducing this burden, to Washington Headquarters Services, Directorate for Information Operations and Reports, 1215 Jefferson Davis Highway, Suite 1204, Arlington VA 22202-4302. Respondents should be aware that notwithstanding any other provision of law, no person shall be subject to a penalty for failing to comply with a collection of information if it does not display a currently valid OMB control number.

1. REPORT DATE **01 JAN 1993**	2. REPORT TYPE **N/A**	3. DATES COVERED **-**

4. TITLE AND SUBTITLE **Abrasion Resistance Evaluation Method for High-Density Polyethylene Jackets Used on Small Diameter Submarine Cables**	5a. CONTRACT NUMBER **N00039-91-C-0072**
	5b. GRANT NUMBER
	5c. PROGRAM ELEMENT NUMBER
6. AUTHOR(S) **Kevin G. Booth**	5d. PROJECT NUMBER
	5e. TASK NUMBER
	5f. WORK UNIT NUMBER
7. PERFORMING ORGANIZATION NAME(S) AND ADDRESS(ES) **Applied Physics Laboratory University of Washington 1013 NE 40th St. Seattle, WA. 98105-6698**	8. PERFORMING ORGANIZATION REPORT NUMBER **APL-UW TR 9303**
9. SPONSORING/MONITORING AGENCY NAME(S) AND ADDRESS(ES)	10. SPONSOR/MONITOR'S ACRONYM(S)
	11. SPONSOR/MONITOR'S REPORT NUMBER(S)

12. DISTRIBUTION/AVAILABILITY STATEMENT
Approved for public release, distribution unlimited

13. SUPPLEMENTARY NOTES
This thesis was submitted in partial fulfillment of the requirements for the degree of Master of Science in Mechanical Engineering to the College of Engineering at the University of Washington.

14. ABSTRACT
A standard off-the-shelf Taber Abraser instrument is used to quantify the abrasive wear resistance of high-density polyethylene jackets on small diameter submarine cables. The procedures developed and used resulted in reliable and repeatable data and form the basis for an evaluation method of abrasive wear resistance. The wear rates of HDPE cable jacket and flat sheet specimens were compared.

15. SUBJECT TERMS

16. SECURITY CLASSIFICATION OF:			17. LIMITATION OF ABSTRACT	18. NUMBER OF PAGES	19a. NAME OF RESPONSIBLE PERSON
a. REPORT **unclassified**	b. ABSTRACT **unclassified**	c. THIS PAGE **unclassified**	**UU**	**88**	

Standard Form 298 (Rev. 8-98)
Prescribed by ANSI Std Z39-18

Abrasion Resistance Evaluation Method
For High-Density Polyethylene Jackets
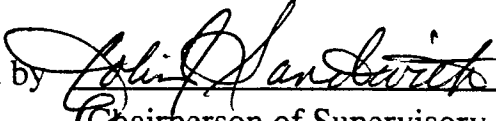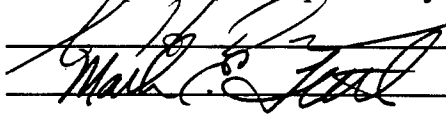Used On Small Diameter Submarine Cables

by

Kevin G. Booth

A thesis submitted in partial fulfillment
of the requirements for the degree of

Master of Science in Mechanical Engineering

University of Washington
1992

Approved by _____
              (Chairperson of Supervisory Committee)

              _____

Program Authorized
to Offer Degree _____ Mechanical Engineering _____

Date _____ *15 December 1992* _____

FOREWARD

This thesis was submitted in partial fulfillment of the requirements for the degree of Master of Science in Mechanical Engineering to the College of Engineering at the University of Washington. Dr. Colin J. Sandwith, Principal Mechanical Engineer at the Applied Physics Laboratory and Research Associate Professor in the Department of Mechanical Engineering, was chairman of the thesis supervisory committee. Financial support for this research was provided by an Applied Physics Laboratory Assistantship and SPAWAR contract N00039-91-C-0072.

ABSTRACT

A standard off-the-shelf Taber Abraser instrument is used to quantify the abrasive wear resistance of high-density polyethylene jackets on small diameter submarine cables. The procedures developed and used resulted in reliable and repeatable data and form the basis for an evaluation method of abrasive wear resistance. The wear rates of HDPE cable jacket and flat sheet specimens were compared. The wear rate of the flat sheet is generally proportional to the number of abrasion cycles, while the wear rate of the cable jacket is proportional to the number of abrasion cycles only after a higher initial, or transient, wear rate. Several factors that affect the wear depths and rates were also investigated. These include the abrasive grit size, the effective coefficient of friction between the abrasive wheels and specimens, the HDPE buildup and coating on the abrasive wheels, and the presence or absence of distilled water covering the cable specimens. Finally, the abrasive energy density is calculated and compared for the different test conditions, i.e., abrasive wheel type, and wet or dry test conditions.

In presenting this thesis in partial fulfillment of the requirements for a Master's degree at the University of Washington, I agree that the Library shall make its copies freely available for inspection. I further agree that extensive copying of this thesis is allowable only for scholarly purposes, consistent with "fair use" as prescribed in the U.S. Copyright Law. Any other reproduction for any purposes or by any means shall not be allowed without my written permission.

Signature _____

Date _____15 December 1992_____

TABLE OF CONTENTS

LIST OF FIGURES

LIST OF TABLES

LIST OF SYMBOLS

A_f	Final wear area at end of 5000 cycle abrasion period.
A_i	Initial wear area at beginning of 5000 cycle abrasion period.
A_r	Real area of contact between two surfaces.
C_L	Assumed contact point of left-hand abrasive wheel on turntable.
C_R	Assumed contact point of right-hand abrasive wheel on turntable.
d	Diameter of abrasive wheel retaining nut.
D	Diameter of abrasive wheel.
E	Energy expended during abrasion period.
F	Friction force defined by shear strength and real area of contact.
f_k	Force component due primarily to kinetic friction.
F_K	Force required to overcome kinetic friction and maintain constant velocity of an object
F_L	Force applied to the turntable by the left-hand abrasive wheel.
F_R	Force applied to the turntable by the right-hand abrasive wheel.
f_s	Force component due primarily to static friction.
G	Generalized normal force.
h	Measured wear depth.
i	Summation index identifying each wear region.
L	Length of wear region on cable specimens.
μ_E	Effective coefficient of friction.
μ_K	Coefficient of kinetic friction
N	Force applied normal to the turntable specimen by an abrasive wheel.
n	Number of turntable cycles (revolutions).

O	Center of the turntable, through which the turntable's axis of rotation passes perpendicularly to the plane of the turntable.
Π	Energy density (energy per unit volume).
Π_σ	Stress-normalized energy density.
r	Radius of the cable specimen.
R	Radius to the center of the wear path on the turntable specimens.
s	Shear strength of material.
S	Sliding distance.
V	Total volume of abraded material
v	Volume of abraded material at each wear region.
W	Weight

ACKNOWLEDGMENTS

DEDICATION

To my parents,

whose support is never ending.

And to Jonathan,

who had to endure the crises that occurred daily,

who supported me to the very end,

and without whom I would have given up long ago.

Chapter 1

INTRODUCTION

Background

Electro-optical submarine cables must meet many requirements in order to sustain a long service life and maintain structural integrity in harsh ocean environments. The cable jacket must be resistant to abrasion and wear and remain water-tight to prevent corrosion of the underlying electrical shield and structural cable components. Abrasion and wear of the cable jacket are caused by the cable laying and handling equipment during cable deployment and by cable strumming due to tidal motions and currents in the water after cable deployment. Original hemp and tar, and solid paper cable coatings, or jackets, are being replaced with polymeric materials. Polymers are being used because of their material properties, corrosion resistance, wear resistance, low cost, and ease of manufacture.

In the 1980s, fiber-optic cable systems became operational, and in 1988 a new generation of submarine cables was laid across the Atlantic [1]. The new generation of submarine cables is generally lighter weight than the predecessors. The new cables, as shown in Figure 1, can consist of a fiber-optic core structure surrounded by helically wound steel strands inside a welded steel or copper tube. The tube is encased in a continuous layer of water–resistant, electrical insulation, in this case medium-density polyethylene, which is surrounded by steel shielding. Finally, a continuous jacket of a polymer material is extruded over the steel shielding. In shallow waters around harbors and fishing areas, the submarine cables often have helically wound steel armor wires added, as an additional strength member, and may be buried in the ocean floor to pro-

tect the cable from anchors and fishing gear. Deep water cables are often laid on the surface of the ocean floor [2].

Insulation

Shielding

HDPE Jacket

Fiber Optic Core
Structure

Submarine Cable Cross−Section
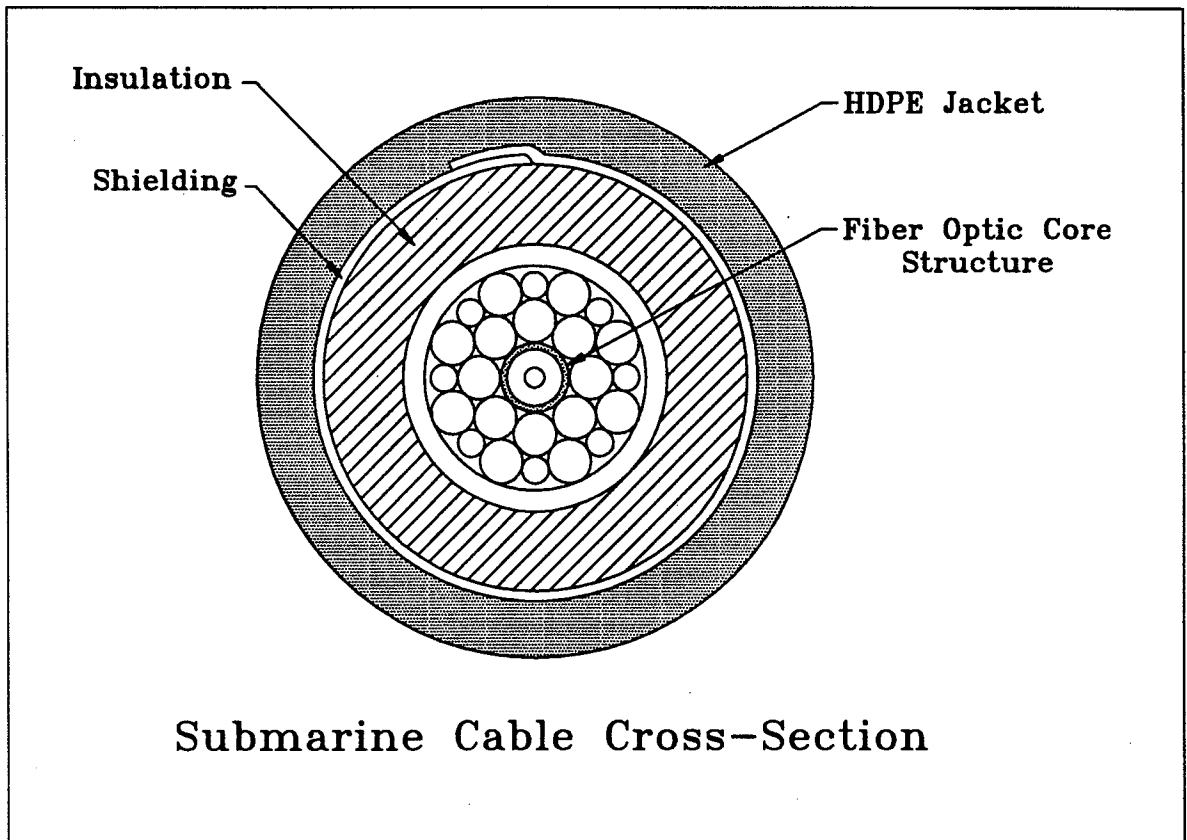
Figure 1. Cable cross-section showing construction details of an electro-optic, submarine cable.

One polymer used extensively for cable jackets in deep ocean applications is high-density polyethylene (HDPE). The high electrical resistance, low specific weight and low frictional coefficients of HDPE are all advantageous material properties for cable jackets. The strength and toughness of HDPE become degraded when the polymer is exposed to sunlight due to the polymer's absorption of ultra-violet light and subsequent photodegradation. This photodegradation

is not limited to the surface of polyethylene, but can affect the bulk material. However, ultraviolet-absorbers or ultraviolet-scattering pigments, such as carbon black, when added to the HDPE during manufacture can slow the photodegradation of HDPE. The addition of carbon black makes polyethylene black and opaque [3].

The extensive use of polymers, specifically HDPE, in critical undersea applications demands a better understanding of the wear mechanisms in order to more accurately predict and compare the service life of various manufacturers' cables. In this thesis, wear is defined as the accumulated loss of material due to the relative motion of two contacting surfaces.

Several tests have been developed to measure the wear resistance of materials. The tests are generally classified by the geometry of the contacting surfaces (cylinder-on-cylinder, pin-on-disk, plane-on-plane), the presence or absence of abrasives, and either lubricated or non-lubricated conditions. Adhesive, or sliding, wear is defined as wear due to the relative motion between two contacting surfaces without abrasives present in the contact area. The contact area is the area where the two surfaces come together on a macroscopic scale, also referred to as the "apparent area" of contact or as the "contact zone." When abrasives, either loose or bonded, are present in the contact area the wear is classified as abrasive wear. Bonded abrasives are made of small, relatively hard particles, called abrasives, that are held in an epoxy resin and can be made into sheets or other more complicated shapes, such as disks, cylinders or cones, depending on the intended application.

Abrasive wear test methods use either loose abrasives sliding between contacting surfaces, loose abrasives impacting the surface as in erosion tests, or bonded abrasives rubbing against the test surface. Abrasion testing using bonded abrasives has been standardized for the abrasion resistance of plastics in JIS-K-7204 as "Testing method for abrasion resistance of plastics by an abrasive wheel," and a Taber abraser is specified in ASTM-D-1044, "Standard test method for resistance of transparent plastics to surface abrasion." However, these standard test methods are limited to flat sheet specimens, in contrast to the round, cylindrical shape of cable jackets.

Problem Statement

Abrasive wear is a complex process of energy transfer by friction, adhesion, shearing, plastic deformation, tearing, fracture, and fatigue [4 and 5]. Abrasive wear is further complicated by secondary interactions between the abraded fragments and the abrading materials or surfaces [6]. The material's properties, as well as these secondary interactions, can affect the abrasive wear rate. The current theories of abrasion and wear for polymers are not reliable for quantifying or predicting the wear rates in many practical applications, including the abrasive wear of cable jackets in the deep ocean. In addition, the coefficient of friction may affect the abrasive wear rate. However, standard friction test methods are not applicable to the finished cable jacket. The effect of the jacket's coefficient of friction, therefore, has not been adequately investigated with respect to the cable geometry.

The objective of this thesis is to better understand and explain, using the thick abrasive wheels and Taber Abraser machine, the abrasive wear mechanisms of the HDPE cable jackets, the relationship between the effective coefficient of friction and the energy density required to produce a specific wear rate, and the relationship between wet and dry test conditions. In addition, a comparison is made of the wear rates between flat sheeting and the round, cylindrical cable shape in an effort to determine the effect of the round cable shape on the abrasive wear rate of the cable jackets. The final goal is to develop an abrasion resistance test methodology that will provide a quantifiable measurement of the abrasion resistance of the manufactured cable jacket material in order to compare different manufacturers' cable jackets.

Chapter 2

LITERATURE SURVEY

Submarine Cables

The deep water cables laid on the ocean floor are subject to abrasion and wear caused by rubbing against sand, rocks, gravel, and crustaceous matter. Ocean currents perpendicular to the cable can cause a strumming or oscillatory motion of the cable. This cable motion may cause rubbing and abrasion to occur at the stress bearing points of cable lengths that are suspended between rock outcroppings, cliff walls, or other protuberances on the sea floor, as is shown in Figure 2. The Naval Civil Engineering Laboratory [7] suspects that

Bearing Point

Bearing Point

Rock Aggregate

Rock Aggregate

Sea Floor

Undersea Cable

Sea Currents
Perpendicular to Cable Axis

One Mechanism of Cable Abrasion
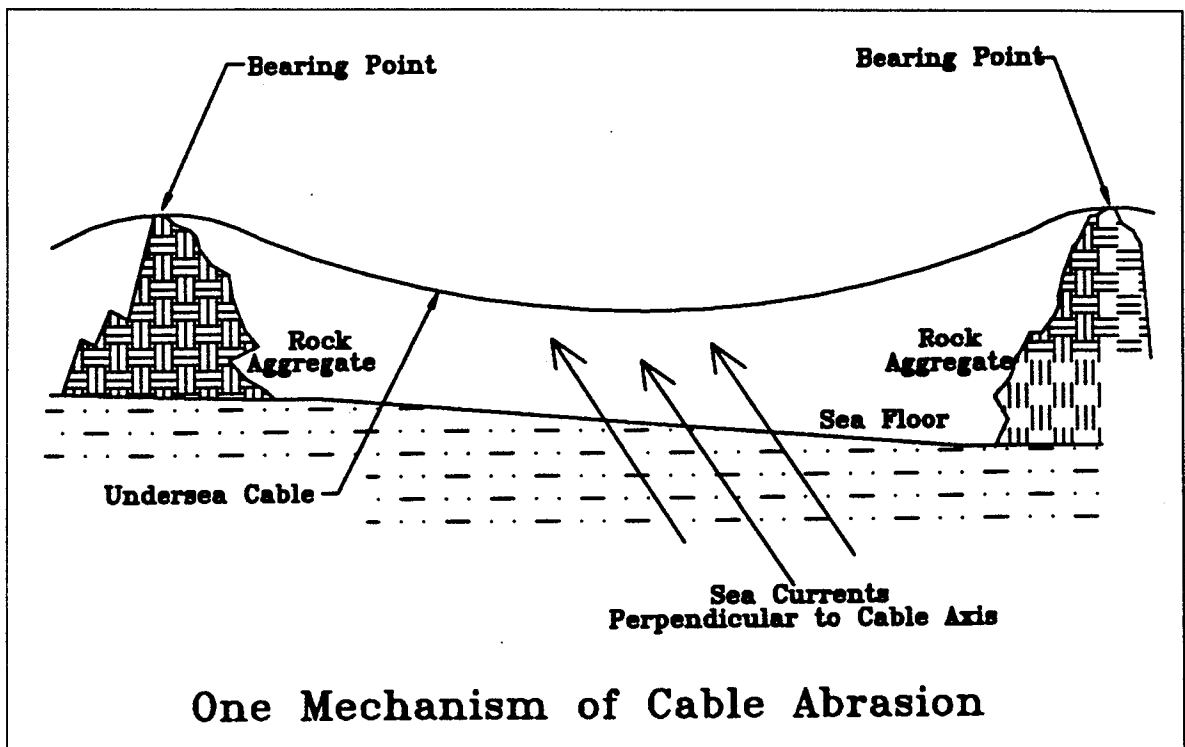
Figure 2.   Illustration of cable, deployed on the sea floor, showing suspension between rocks which is a possible abrasive wear mechanism.

abrasion, caused by cable strumming and rubbing, is a likely failure mode in submarine cables.

Expected cable failures due to cable strumming and rubbing are believed to be preceded by a period of abrasion due to the cable's motion or some other cause. The expected failure occurs when the abrasion penetrates through the cable jacket to the underlying steel shield. Any through-the-jacket damage can allow seawater to propagate along the cable around, under and thru the steel shield causing corrosion and penetrations or holes (leaks) through the insulation. Any seawater leakage and resulting corrosion can eventually cause a total system failure by a loss of electrical continuity, or a loss of insulation (electrical isolation) caused by a seawater leak between the high-voltage conductor and surrounding seawater, or a decrease in cable strength, and finally total failure of the cable's integrity [8].

Friction

It is well known that when two surfaces are brought together and make contact, the actual area of contact is smaller than the apparent area of contact. The actual area of contact is also called the real area of contact. The surface of either material can be thought of as a landscape of hills and valleys, and the hills, or asperities, become the points of contact forming the actual or real area of contact between the two surfaces [9, 10, 11, and 12].

The Coulomb theory of friction, which is based on the mechanical engagement of asperities between surfaces, can account for static friction but does not account for the loss of energy during sliding. When two materials are in sliding contact, the asperities of one surface are not continually ascending the asperities of the other surface, but instead must first ascend one side and then descend the other side of the asperity [9].

In contrast to the Coulomb friction theory, the current theory of friction is based on adhesion of two surfaces. It has been shown that when two chemically clean and molecularly flat mica surfaces (produced by cleaving) are brought together, the energy required to recleave the mica along the same surfaces is only 15% less than the energy that was required for initial cleavage. Thus it is thought that when two surfaces are brought together and make contact, deformation of the asperities occurs and, subsequently, bonds form between the contacting asperities of the two surfaces. The adhesion theory of friction defines the force due to friction as the force required to shear the bonded, or adhered, asperities [9].

However, not all investigators agree with the adhesion theory of friction. Bikerman [10] suggests that the presence of weak boundary layers of air, water, and other contaminants prevents adhesion from occurring between the two surfaces. He states that friction, instead of being the result of adhesion between the two surfaces, is due to deformation of the contacting asperities. However, as has been shown in experiments using molecularly flat mica surfaces, D. Tabor points out in his comments to Bikerman's paper that even with the presence of an adsorbed monolayer of water on mica surfaces, adhesion forces,

although small, can still be measured.

Assuming the adhesion theory of friction to be correct, the friction force **F** is related to the shear strength, s, of the weaker material and the real area of contact A_r as

$$\mathbf{F} = s\,A_r\,.$$

Sliding of one surface over the other can also cause the asperities of both materials to shear and deform, as in the case of sliding between two materials of equal shear strengths [11].

The energy associated with wear is generally thought to consist of three types: mechanical, chemical, and thermal. Mechanical energy is the energy expended when asperities of one or both surfaces are deformed due to shearing. For contacting materials where one material is harder or has a greater shear strength than the other, the asperities of the harder material plow through the asperities of the softer material. Plowing causes deformation of the softer material to occur and, in the process, expends mechanical energy [11].

Chemical energy is associated with the work done in breaking the intermolecular and atomic bonds formed between the contacting surfaces. The strongest bonds formed are the covalent, ionic, or metallic bonds. In the absence of these types of strong bonds, or chemical reactions between surfaces, Van der Waal's forces must still be overcome. However, Van der Waal's forces are much weaker than the forces developed by the previous three bond types [11].

Thermal energy in the form of heat is generated by the relative motion and friction between the two contacting materials. The heat generated can cause localized melting, welding, swelling, shrinking, and cracking which can either increase or decrease the friction and wear between the materials, in addition to being a mechanism for the loss of energy to the surroundings [11].

Wear

Wear is defined as the accumulated loss of material due to the relative motion of contacting surfaces, and is characterized by a loss of material volume or a change in the surface properties, such as a change in the surface roughness, a change in the surface texture, or a loss of optical transparency as measured by light transmissivity of the material. Wear is a complicated phenomena and is often caused by, or the result of, one or more of the following mechanisms: adhesion, tearing, cutting, plastic deformation, fatigue, surface fracture, corrosion, and melting. Wear usually results due to complex combinations of the above mechanisms, and rarely results from only one of the mechanisms alone [11].

Wear is often divided into two broad classifications: mild wear or severe wear [12], particularly for wear of metals. The classification of mild versus severe wear, although widely adopted and somewhat useful as a general material selection criteria for some applications, is criticized as being quite arbitrary. An

alternative method is to classify wear according to the mechanism involved, such as tearing, spalling, or fracture wear. However, wear often results from more than just one isolated mechanism, and thus this classification becomes difficult to apply when more than one wear mechanism is a significant cause of wear. A generally accepted and more descriptive classification of wear is based on the presence or absence of abrasive particles within the wear region. Abrasive particles, or abrasives, are generally considered to be any substance that is harder than the material that is subject to wear. Using this classification method, wear is classified as either adhesive or abrasive wear [12].

Adhesive wear, often called sliding wear, is defined as wear that occurs due to the relative motion between surfaces without abrasives, or abrasive particles, in the contact zone. Abrasive wear, on the other hand, is defined as wear that occurs due to the relative motion between surfaces with abrasives in the contact zone. Abrasive wear is further divided based on the type of abrasive: loose abrasives, bonded abrasives, and erosive, or impact, abrasives. Adhesive and abrasive wear are both affected by the presence of lubricants, the nature of relative motion (unidirectional or reciprocating), the combination of surface conditions (smooth on smooth, rough on smooth, or rough on rough) and geometrical shape (plane on plane, cylinder on plane, or cylinder on cylinder), and the types and combinations of contacting materials [12].

Abrasive Energy Density

Energy density, when defined as the energy expended per unit area, was used to evaluate the effectiveness of abrasives for removing marine fouling from a ship's hull by Sandwith and Breiwick [13]. They used different sizes of black-powder charges to propel abrasives toward a hull. The area of impact was not constant, but instead varied with the type of abrasive, amount of blackpowder used, and the distance between the hull and gun barrel. In their tests, the mini-mum energy density indicated the optimum parameters to remove the marine fouling for the abrasives tested. When cables abrade, however, the abraded area may not remain constant due to the cylindrical cable geometry. Generally the length of the cable abrasion area remains constant; thus the area of abrasion is related to the volume of abraded material by the width of the abrasion area. For this investigation of cable abrasion, abrasive energy density is defined as the energy expended divided by the volume of material removed.

Polyethylene Material Properties

Generally, polymer crystallinity is directly related to density and molecular weight, and molecular weight is inversely related to the polymer's melt index. Test results presented by Deanin and Patel [14] suggest that abrasion resistance of polyethylene is directly related to indentation resistance, tensile modulus, tensile yield strength, and ultimate tensile strength. They found that polyethylenes with a high degree of crystallinity had greater indentation resis-

tance, higher tensile modulus, higher tensile yield strength, and higher ultimate tensile strength than did polyethylenes with a lower degree of crystallinity. The polyethylenes with a higher degree of crystallinity were found to have a greater resistance to abrasion than the polyethylenes with a lower degree of crystallinity. Similarly, they found that, at high molecular weight, tear strength increased with crystallinity and tear strength is directly related to abrasion resistance. A Tabor Abraser and weight loss due to abrasion were used to test and measure the abrasion resistance of the polyethylene flat sheet specimens.

Professor Sandwith [15] believes that toughness of the material may be an important factor in abrasion resistance. Deanin and Patel found that elongation was not related to wear resistance, but tear strength and ultimate tensile strength were both directly related to abrasion resistance. This tends to support the belief that toughness of the material may have a direct impact on abrasion resistance.

Deanin and Patel found very little correlation between the coefficient of friction of the polyethylene and its structure, properties, or abrasion resistance. They used ASTM D1894, a standard test method for plastic on plastic, to make their coefficient of friction measurements. They contributed the lack of a proportional relation between coefficients of friction and the polyethylene's structure, properties, and abrasion resistance to possible "unknown compounding additives or low-molecular-weight waxy fractions." Both additives and waxy fractions can greatly affect the abrasion resistances and frictional properties of polymers. In their tests Deanin and Patel were using resilient abrasive wheels (abrasive particles in a elastomeric bonding matrix) to wear the polyethylene.

Bahadur and Tabor [16] have investigated the role of fillers and thin transfer films on the frictional coefficients and wear rates of high-density polyethylene (HDPE). Their results show that, depending on the filler used, the wear of HDPE can change dramatically. Some fillers, such as CuS in a 30% CuS to 70% HDPE ratio, drastically reduced the wear rate of HDPE sliding on a rough steel surface without affecting the HDPE-on-steel coefficients of friction. Other fillers, such as polar graphite, caused an increase in both friction and wear. They found that the addition of wear-rate-reducing fillers actually strengthened the HDPE, which resulted in lower wear rates. Toughness values of the strengthened HDPE were not reported.

The role of dry or wet conditions on wear produced in ultra-high molecular weight polyethylene (UHMWP) sliding against stainless steel with different surface roughness values was investigated by Dowson et al. [17]. In the wet condition tests, the test surfaces were submerged in distilled water. They found the presence of distilled water inhibited the formation of a transfer film (a thin layer of abraded material that adheres to the abrading surface), which caused an increase in wear factors compared to the dry condition tests. Dowson et al. used wear factors, defined as the volume loss due to wear divided by the energy expended (inverse energy density), to present their wear data and results. A larger wear factor represents a greater amount of wear when the energy expended is equal.

Taber Abraser

The Taber Abraser is a standardized test instrument used for evaluating the abrasion resistance of sheet materials. The test material is placed on a platform that is attached to a motor. The motor rotates the platform, or turntable, at a constant angular velocity. Two abrasive wheels, each mounted on an independent pivoting arm, contact the test material, as shown in Figure 3. Figure 3 is a picture of the two-station Taber Abraser, model 5150, as modified to accept cable specimen thicknesses. The turntable shown on the right-hand station contains the HDPE sheet specimen, and the turntable on the left-hand station contains cable specimens.

Weights can be added to the pivoting arms to set the normal force exerted by the abrasive wheels onto the test material. The rotation of the turntable produces rotation of the abrasive wheels, but, due to the location of the contact point between the abrasive wheels and the turntable, sliding also occurs between the wheels and the test material, producing abrasion and wear.

The Taber Abraser is used in several standard test methods as prescribed by the American Standards for Tests and Materials: ASTM F510–81, Resistance to Abrasion of Resilient Floor Coverings; ASTM D4060–90, Abrasion Resistance of Organic Coatings by the Taber Abraser; and ASTM D1044–91, Test for Resistance of Transparent Plastics to Surface Abrasion. The Taber Abraser is also used to evaluate the wear resistance of wire coatings, fabric, concrete, and paint. Recently and in contrast to its previous uses, the Taber Abraser has been used to evaluate the abrasion resistance of cable jacket materials.
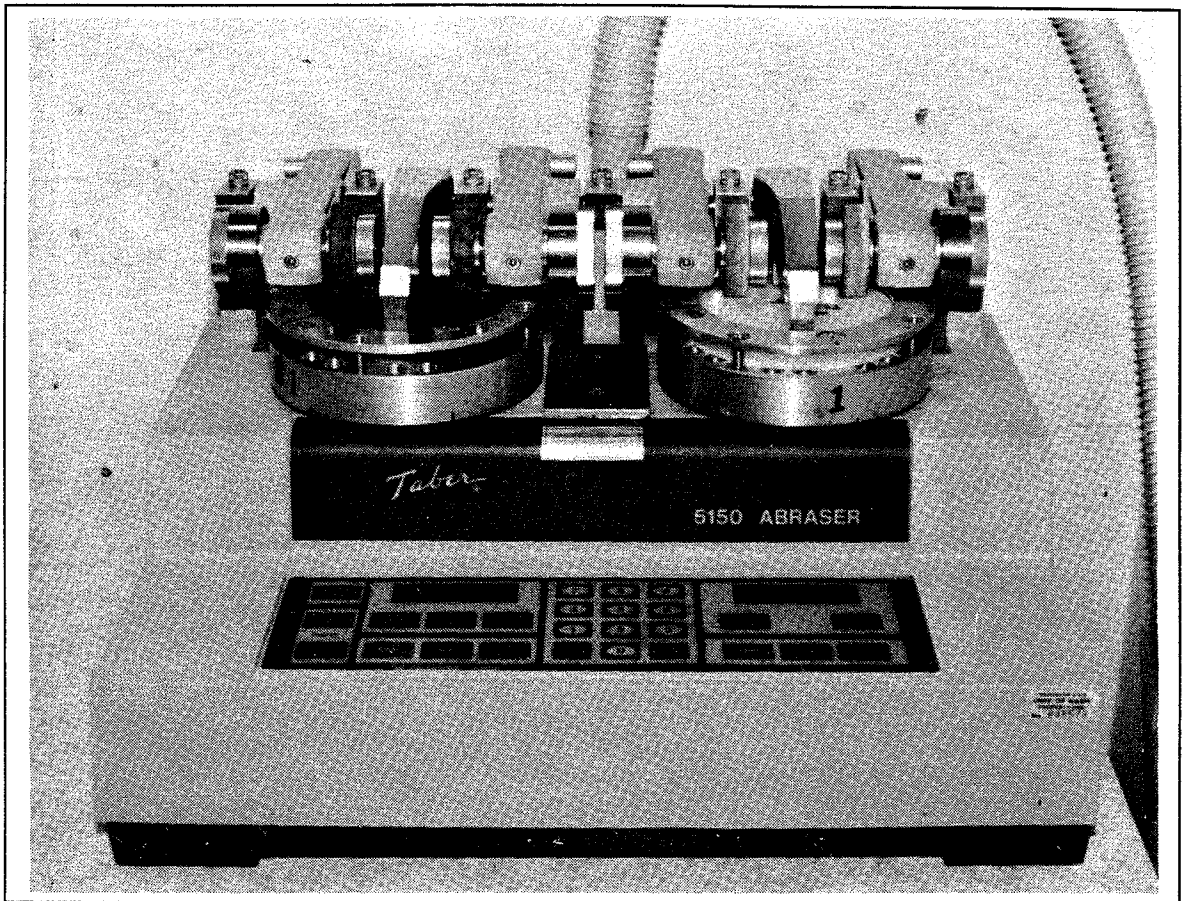
Figure 3. Modified Taber Abraser, model 5150, fitted with turntables and abrasive wheels.

Sandwith *et al.* [18] investigated the use of a slightly modified Taber Abraser to evaluate the abrasion resistance of cable jackets. Their long-term objective was to develop a standard test method to measure and compare cable jacket abrasion resistance. They determined that the Taber instrument could be used to evaluate the cables' abrasion resistances; however, the procedures used with the modified Taber Abraser needed refining in order to produce a "useful standard test." Each cable specimen's particular abrasion location(s) had a particular, individual relative motion with respect to the abrasion wheel axis of rotation; thus an abrasion orientation-rotation pattern resulted on the cable speci-

mens within the individual cable rafts. They attributed the variations in results they encountered to the complex orientation-rotation pattern and the variations of the abrasion location lengths on the cable specimens between cable rafts.

The experimental results and analysis by Sandwith *et al.* produced more complicated questions than they answered. For example, how does the non-flat, unsymmetrical surface of the raft affect wear by abrasion? In addition, the effects of the cables' cylindrical shape on the wear rate of the cable jacket were not completely explained. The impetus for the current thesis comes directly from the problems experienced during the investigation conducted by Sandwith *et al.* This thesis attempts to determine the effect of the round, cylindrical shape of the cables on the wear rates produced by the Taber Abraser on the cable jackets. In addition, this thesis compares the effects of dry and wet conditions on the wear rate, examines the effects due to the HDPE buildup on the abrasive wheels, and investigates the relationship between the coefficient of friction and energy density in producing a specific wear rate.

Chapter 3

EXPERIMENT

Objective

The experiments in this thesis are designed to measure the wear rates of the HDPE cable jacket when using a standardized test instrument. The wear rates of the cable samples are compared with the wear rates of flat sheet HDPE in an effort to separate the wear effects due to the different surface goemetries: the flat, even surface of the flat sheets versus the non-flat, uneven surface of the cable rafts. In order to meaningfully compare the results between the flat sheet and cable jacket specimens, the hardness of the different materials is measured.

The wear rates of the cable specimens are compared between dry and wet abrasion test conditions. Dry abrasion test conditions refer to abrasion tests conducted in air at room temperature and humidity. Wet abrasion test conditions refer to abrasion tests conducted with the cable specimens immersed in room temperature distilled water during the abrasive wear test cycles. The purpose of the wet condition tests is to determine if an increase or decrease in wear rates results due to the cables immersion in water.

Then, to determine the power density, or energy per unit volume of abraded material, the coefficients of friction are measured for the flat sheet and cable jacket materials in contact with the two types of abrasive wheels. Using the measured coefficients of friction, the energy density is calculated based on a defined hypothesis. In the following sections, the test samples will be identified, the test instruments and apparatus will be described, the energy density formulation and calculation will be illustrated, and the experiment procedures will be detailed.

Specimen Materials and Preparation

The cables used in this thesis for all cable jacket abrasion and wear tests were received by Professor Colin J. Sandwith, at the Applied Physics Laboratory–University of Washington, in March 1991 from Simplex, Incorporated, as part of the research funded under SPAWAR contract N00039-91-C-0072. Measurements made of the cable's cross-section were within the nominal dimensions as specified in SPAWAR-C-833D Cable, Fiber Optic, Deep Water Trunk [19], and as shown in Figure 4.
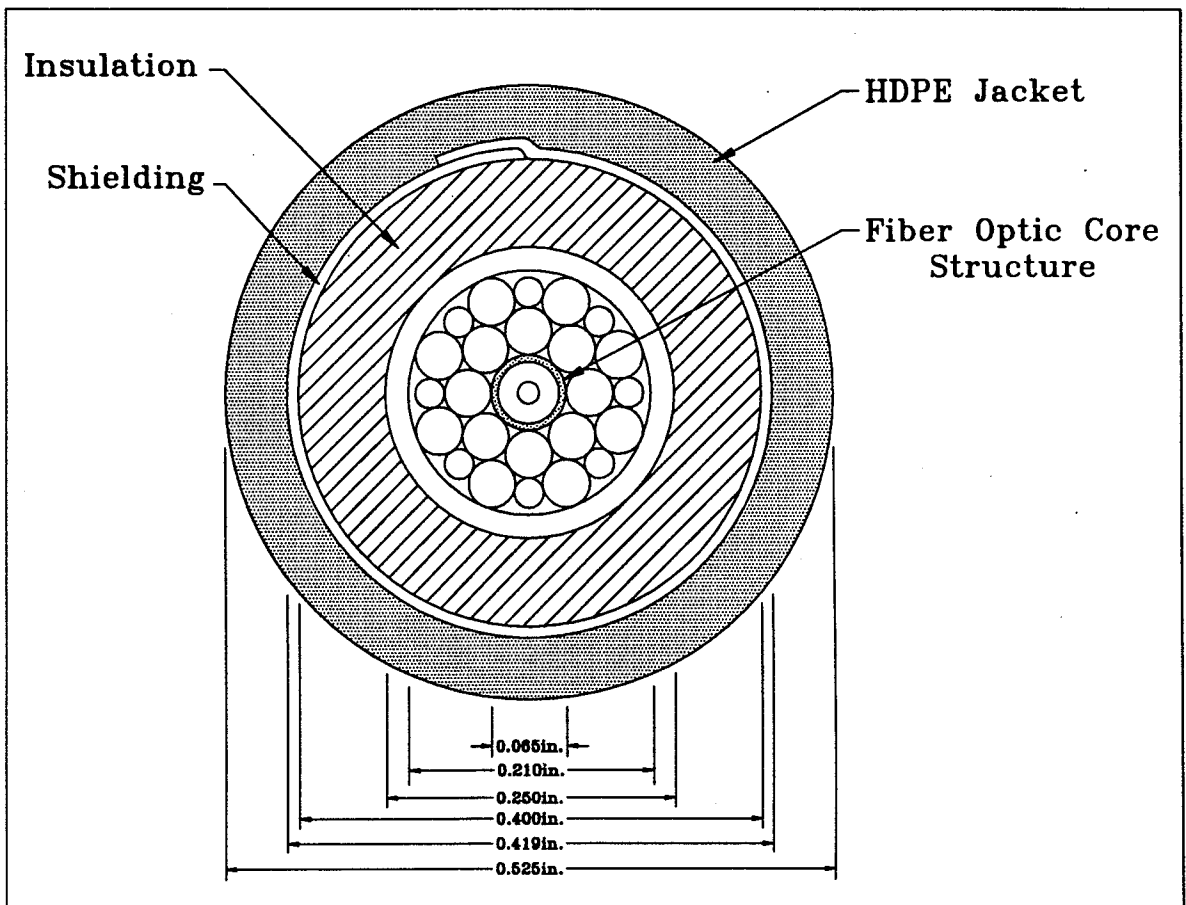
Figure 4. Nominal dimensions of submarine cable used in the abrasion and wear tests on cable specimens.

The HDPE sheeting, used in the flat sheet abrasion and wear tests, was received from Boedeker Plastics, Incorporated, Shiner, Texas, on June 30, 1991, and is 1/8in. thick and opaque white. Using a band saw, five-inch diameter specimens were cut out of the 0.125in. nominal thickness HDPE sheeting. The material properties of the HDPE, as provided by Boedeker Plastics [20], are given in Table 1.

Table 1. Material Properties* of Opaque White, 1/8in. HDPE Sheeting.

Density, g/cm^3	0.955
Tensile yield strength, psi	4,600
Tensile elongation at yield, %	900
Flexural modulus, psi	200,000
Hardness, Shore D	69

*As provided by Boedeker Plastics, Inc.

Test Apparatus

Durometer

Hardness tests were conducted as specified in ASTM D 2240 using a Shore Instrument and Manufacturing Company, Incorporated, Durometer Type D, model XDMXHAF durometer, serial number 97988. This model of durometer

has a 0.5in. diameter foot, with a sharp 30° included angle indenter with a 0.004±0.0005in. indenter tip radius, and is made to conform with ASTM D 2240. The Shore durometer comes equipped with a calibration test block. If the durometer is properly calibrated, it will measure a hardness of 50 (on a scale of 100) when used with the calibration block. This model of durometer has an indicator needle that holds the maximum reading obtained during each hardness test.

All values reported in the results section of this thesis are the maximum reading values obtained, using the hand-held durometer, because of the viscoelastic nature of HDPE. This viscoelastic property allows the HDPE to creep and flow away from the hardness indenter, which causes the hardness reading from the durometer to decrease with the length of time of applied pressure from the hardness indenter. Prior to conducting hardness tests, the durometer's calibration was verified using the calibration test block supplied by the manufacturer, and a proper measurement of 50 was obtained. The hardness test specimens were conditioned at room temperature and standard atmospheric pressure in accordance with standardized test procedures.

Taber Abraser instrument

The Taber Abraser model 5150 used in the experiments is a standard industrial instrument used to test the abrasion resistance of flat sheet materials. The sheet material is secured to a motor driven platform, or turntable. Abrasive

wheels are mounted on each of two individually pivoting arms and contact the turntable at symmetric points. Two types of abrasive wheels with different abrasive sizes were used: Calibrase H-18 vitrified 180 grit and Calibrase H-22 vitrified 80 grit. Weights, attached to the pivoting arms, set the nominal normal force applied by the abrasive wheels to the test substrate. In order to accommodate cable specimens the standard turntable and pivoting arms have been modified to accept specimens up to 20.0mm in thickness. The Taber Abraser instrument removes the loose abraded material by means of two vacuum nozzles. The two vacuum nozzles suck the loose material from the specimens. The nozzles are located such that the bulk of the loose debris is removed after contact between the specimen and an abrasive wheel and prior to the next contact. During wet abrasion test conditions, the vacuum nozzles are deactivated. The accumulation of abrasive particles is prevented by changing the water used during the tests. The water is changed every time the abrasive wheels are exchanged with new or resurfaced wheels.

A plan view of the turntable, including the contact locations of the abrasive wheels, is shown in Figure 5. Point O is the turntable rotation axis. Point C_L is the assumed turntable contact point for the left-hand abrasive wheel and point C_R is the assumed turntable contact point of the right-hand abrasive wheel. Because the abrasive wheels have a finite width, the contact points C_L and C_R, as shown in Figure 5, are assumed to be at the midpoint of the abrasive wear path.

The abrasive wheel forces, F_L and F_R, acting on the turntable are shown, in Figure 5, at the contact points C_L and C_R between the abrasive wheels and the
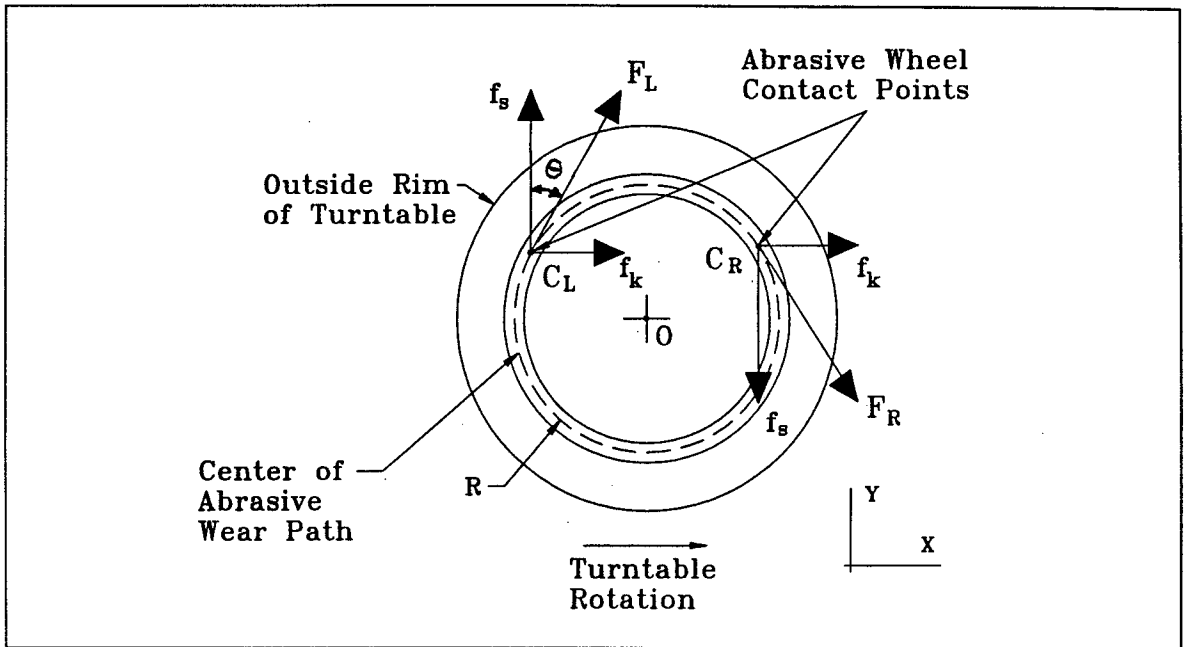
Figure 5. Contact points and forces acting on the turntable platform.

turntable. Also shown are the force components, relative to a local x-y coordinate system as shown in Figure 5 with the origin at point O, of the resultant forces F_L and F_R.

The y-components of F_L and F_R represent the reactions of the force components that result in the abrasive wheels' rotation. Because the abrasive wheels are supported by roller and thrust bearings, rotational drag is assumed to be negligible compared to the applied static rolling friction forces. Therefore rotation of the abrasive wheels is produced by static rolling friction; thus the y-components are due primarily to static friction forces, and are labeled as f_s.

The rotation of the turntable causes an abrasive rubbing action between the sheet material and the abrasive wheels because the abrasive wheels' bearing rotation axis is perpendicular to the y-axis and is a finite distance along the y-axis

away from the center of the turntable (point O). The x-components of F_L and F_R are the force components that result from sliding. The x-components are therefore due to sliding kinetic friction forces applied to the turntable by the abrasive wheels, and are labeled as f_k.

The abrasion and wear produced by the rolling (static) friction forces between the abrasive wheels and the specimen are assumed to be negligible compared to the abrasion and wear associated with the sliding motions and kinetic friction forces. The sliding of the abrasive wheel's surface particles produces cutting, deformation, shear, tearing, and fracture of the HDPE due to the plowing of the abrasive particles into and through the HDPE. These mechanisms of abrasion produce greater, faster wear rates (an order of magnitude, or more, greater) as compared to the fatigue mechanism of wear which is the primary wear mechanism associated with rolling of the abrasive wheels.

Friction force measurement apparatus

The friction between the abrasive wheels and the specimens is a combination of static and kinetic friction. At no time, during an abrasive test when the abrasive wheel is in contact with the test specimen and the turntable is rotating, does either pure static friction or pure kinetic friction exist. Both types of friction are coupled, due to the design of the Taber instrument. Generally, the static friction produces the rotation of the abrasive wheels and the kinetic friction produces the abrasion and wear of the test specimen's surface.

Due to the design of the Tabor instrument and cylindrical shape of the cable specimens, contact between the abrasive wheel and cable specimen varies in width. At the beginning of each abrasion test, the contact varies from nearly a point to the full width of the abrasive wheel, depending on the angle of attack, or angle of contact, formed between the cable's longitudinal axis and the abrasive wheel's rotational axis. Nearer to the end of the abrasion test, the contact continues to vary from the width of the abrasion area (which is a function of the depth of abrasion) to the width of the abrasive wheel. The varying contact point between the abrasive wheel and cable specimen causes the direction of the vector representing the frictional force to also vary slightly, depending on the angle between the longitudinal axis of the cable specimen and the rotational axis of the abrasion wheel.

Because of the variations in contact areas and frictional force directions, and because standardized friction measurement methods are not readily adaptable for use with the cable specimens, an effective coefficient of friction is calculated from frictional forces that are measured using the apparatus sketched in Figure 6. The effective coefficient of friction calculation neglects energy losses and fluctuations from any slight frictional force directional variations and temperature fluctuations.

The effective coefficient of kinetic friction is calculated from measurements of the force required to just stop and prevent further abrasive wheel rotation as produced by the rotating turntable. Once the abrasive wheel has stopped, only sliding, or kinetic, friction is occurring; thus an effective sliding, or kinetic, friction force, which produces the primary abrasive mechanisms, can be measured.
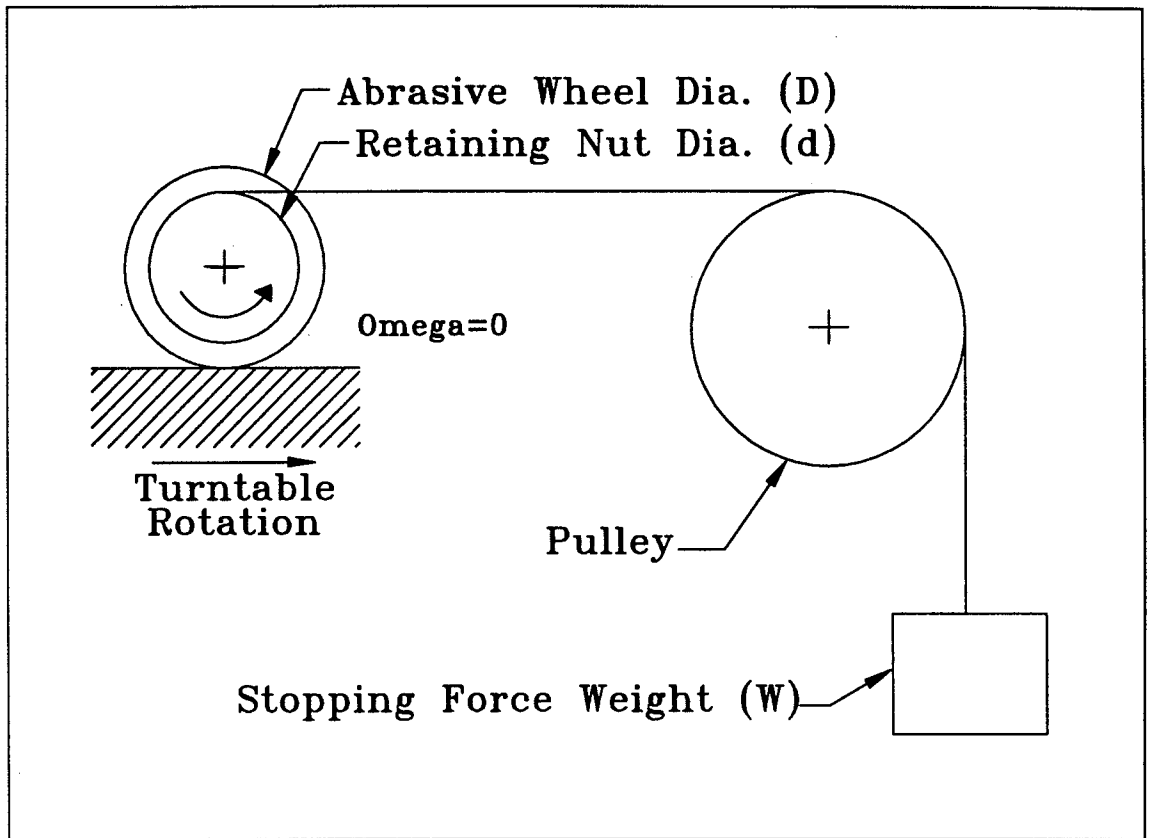
Figure 6. Friction force measurement apparatus.

Wear depth measurement stand

Wear depth measurements are macroscopic measurements of the thickness of material removed by the abrasive wheels. These measurements are a quantitative measure of the abrasion and wear that the cable jackets are subjected to in a specific number of turntable, or abrasion, cycles. Every 5000 turntable, or abrasion, cycles is referred to as an abrasion period. The actual thickness of material removed, or depth of wear, per abrasion period is calculated by subtracting the wear depth measurement made at the end of the previous abrasion period from the wear depth measurement made at the end of the

current abrasion period.

Wear depth measurements are made using a dial micrometer attached to a rigid stand and platform. Initial depth measurements are recorded when the specimens are first loaded and secured into the modified Tabor turntables. The initial measurements provide a zero wear depth, or initial depth, point of reference. This initial depth measurement is subtracted from the depth measurement made at the end of the first abrasion period to find the wear depth of the first abrasion period.

Because of the round cylindrical geometry of the cable specimens, the turntables and the measurement platform are indexed with marks corresponding to the turntable position at which the micrometer stem contacts the highest point on each cable's abrasion locations. Shown in Figure 7 is the depth measurement apparatus. Notice the index marks along the lower edge of the turntable. Subsequent to the initial depth measurements, wear depth measurements are taken at the locations on the turntable indicated by the indexing marks. The wear depth is then recorded at the end of each abrasion cycle until the wear test is completed.

The dial micrometer, a Mitutoyo model number 2904 mounted to a Mitutoyo model 7011-S magnetic-base instrument stand, measures the depth in 0.001in. increments, on a scale of 0.000–1.000in. Twelve individual readings are taken for each abrasion cycle to an accuracy of ±0.0005in. In accordance with standard abrasive wear procedures, the readings for each abrasion cycle

are averaged over all measurement locations in order to produce the average wear rates.
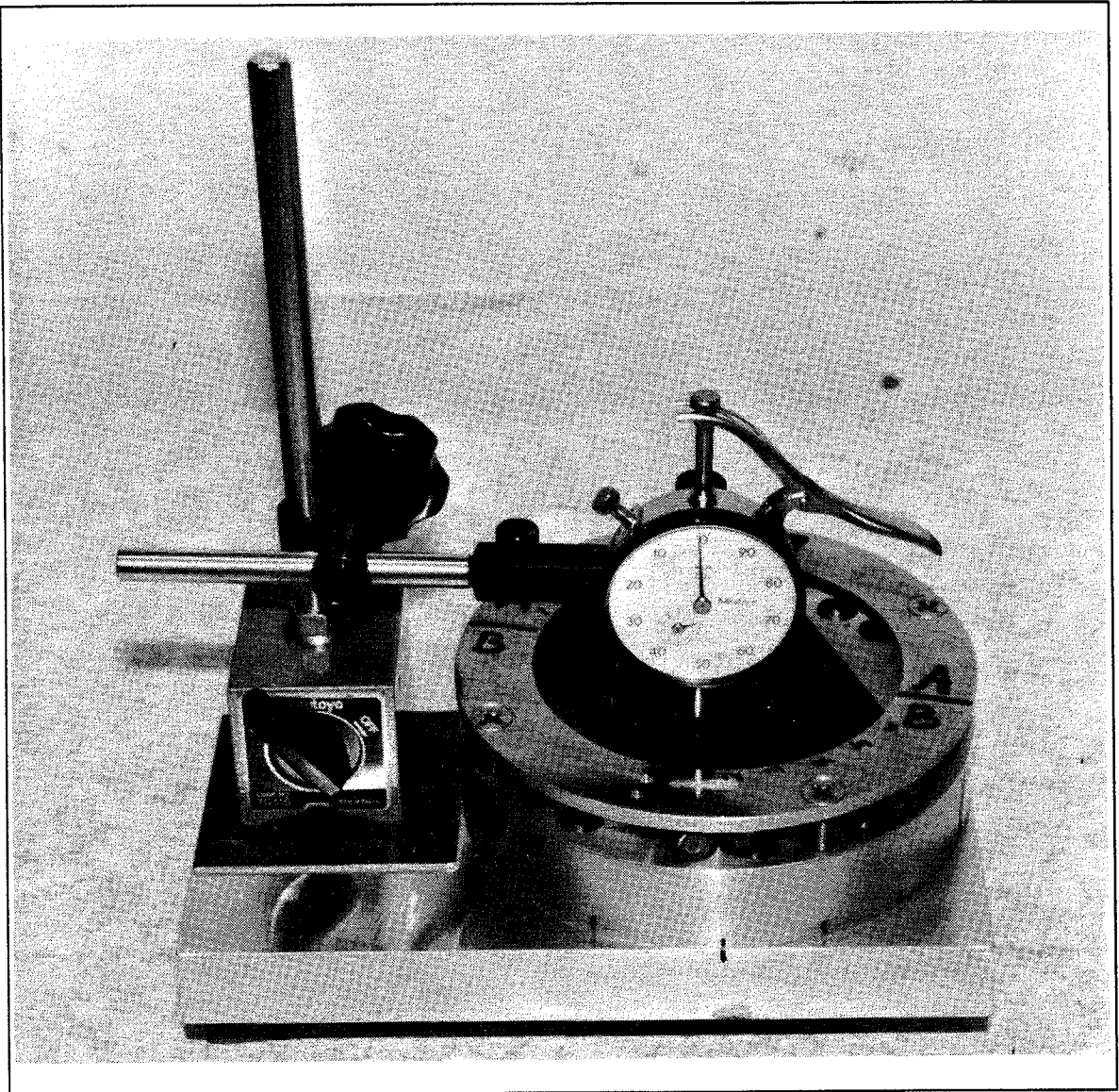
Figure 7. The measurement stand and dial micrometer used for wear depth measurements.

Procedures

Specimen preparation

The cables were received from the manufacturer in approximately 30in. diameter coils. The cables were first uncoiled (generally straightened) and were then cut, using an air-powered abrasive wheel cutter, to make specimens, five inches in length (±0.25in.), which then fit onto the turntable. The use of the abrasive wheel cutter raised concerns regarding the heat it generated in the metal structures of the cables. The heat generated, if allowed to raise the temperature of the entire cable, could cause melting to occur in the HDPE cable jackets. Therefore, each cut of the cable was followed by a five minute waiting period which allowed the cable to cool and prevented a significant rise in the overall temperature of the cable. In order to reduce any effects due to localized melting of the HDPE around specimen ends, the cut ends of the cable are located at least one inch from the abrasion regions, or areas. Thus there should be little effect on the abrasion behavior of the cable jacket due to any localized melting of the HDPE jacket that occurred directly at the cut ends of the specimens.

Six specimens are then placed onto the turntable. The line of contact formed by the contacting sides of the two center specimens is used to position the center two specimens so that this line of contact lies over the diametric centerline of the turntable. The remaining four specimens are packed, two to each side of and next to the two center specimens, as tightly as possible by hand. The specimen retaining ring is then fastened down with screws in order to tightly

hold the specimens in position. The specimen retaining ring is a metal ring that is fastened to the top of the turntable with four screws and is used to hold the test specimens rigidly in position.

Friction force measurements

The sliding friction force is measured using a line secured to and wrapped around the abrasive wheel retaining nut. The line is run over a low friction pulley and the free end is attached to a free-hanging, adjustable weight, as shown in Figure 6. The turntable rotation is started with the abrasive wheel in contact with the test specimen. Then the stopping force weight is slowly increased until the abrasive wheel's rotation is stopped, and the turntable continues to rotate at constant angular velocity. The weight required to prevent the abrasive wheel rotation is measured using a Sartorius electronic scale, to ±0.01g precision.

The friction test is repeated several times for each specimen, abrasive wheel, and test condition. The coefficients are calculated for resurfaced, or new, wheels and for used, or "full," wheels. Used, or "full," wheels are abrasive wheels that have been subjected to abrasive cycle use and the buildup of HDPE has not been removed. Figure 8 shows a new abrasive wheel and a used, or "full," abrasive wheel. The used wheel has been subjected to 5000 turntable cycles of abrasion on cable specimens.
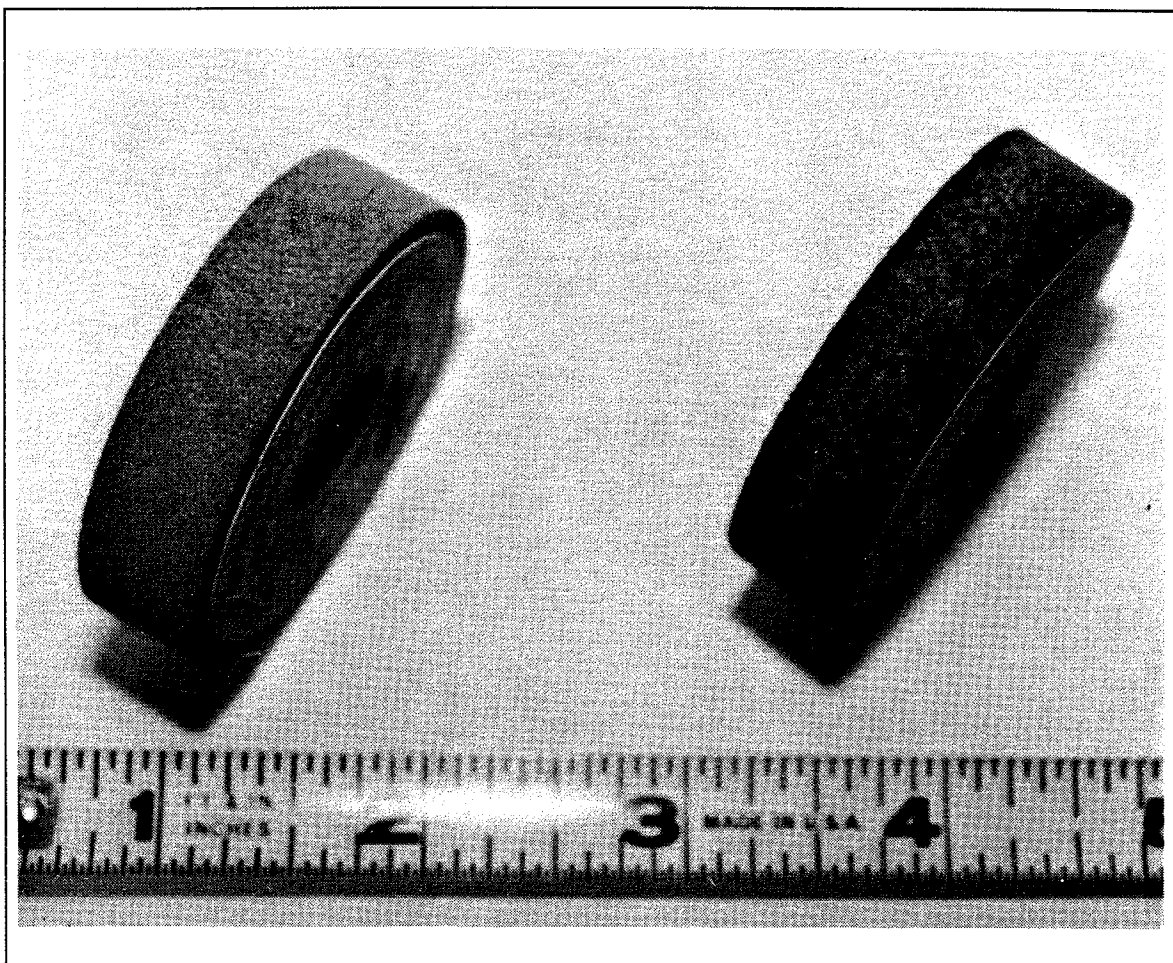
Figure 8. New, resurfaced, abrasion wheel (left) and used abrasion wheel (right). Used wheel was subjected to 5000 turntable cycles.

After the initial test, each subsequent test is considered a valid test only if the contact point is at a different location on the abrasive wheel from any of the previous tests. This prevents any significant buildup of HDPE from occurring in any one location on the abrasive wheel, which could result in a lowering of, or decrease in, the measured stopping force weight (due to a lower coefficient of friction between HDPE and HDPE than between abrasive and HDPE).

Wear depth measurements

The turntable, containing the specimens, is placed on the depth measurement stand, as was shown previously in Figure 7. The turntable is rotated, by hand, and measurements are made of the initial maximum heights of the cable specimens at each abrasion location. These initial measurements become the initial depth measurements, or zero-abrasion-depth measurements. The turntable is indexed, during the cable measurements, to the measurement platform's reference mark. The turntable is therefore marked with each measurement location corresponding to the maximum initial heights of the cable at each abrasion location. All measurements are recorded to an accuracy of ±0.0005in., using the dial micrometer.

Next, the turntable and specimens are placed on the Taber instrument. New, or resurfaced, abrasive wheels are mounted and the Taber Abrader is programmed for the number of complete revolutions (cycles) of the turntable that is to occur. The number of turntable cycles, the type and identifying number of abrasive wheels, the date, and the start time are recorded. The vacuum nozzles are adjusted so that there is adequate clearance between the nozzles and the specimens and, just prior to initiating the abrasion test, the abrasive wheels are lowered onto the test specimens and the Taber Abraser's motor is started (the motor rotates the turntable).

Two methods are used to determine when to replace a set of abrasive wheels with a "new," or resurfaced, set. In the first method, referred to as the wear criterion, the abrasive wheels are replaced only when the change in wear depth, at

half of the wear measurement locations, is less than 0.001in. In the second method, referred to as the cycle criterion, the abrasive wheels are replaced after every 5000 turntable revolutions, regardless of the amount of wear that occurred during the abrasion cycle. Thus for the cycle criterion, each abrasion cycle of 5000 turntable revolutions begins with a new set of abrasive wheels.

The wear criterion was used in a previous study by Sandwith *et al.* [18] but I suspected that this method of changing the abrasive wheels may have been a contributing cause to their enigmatic, or unexplained, variations in results because, after performing several tests using the wear criterion, I noticed that the wear rates observed with new, or resurfaced, abrasive wheels were higher than with wheels that had buildups of HDPE adhered to the abrasive surface. It appeared that there were distinct periods of high wear rates followed by decreasing wear rates that kept repeating at varying intervals throughout the test. The repetition of high-to-low wear rates could be correlated with the changing of the abrasive wheels. Thus I investigated the effect of the HDPE buildup, or filling of the abrasive wheels, on the wear rates.

The cycle criterion was developed as a means of changing the abrasive wheels in a more consistent manner and as an effort to produce fewer unexplained variations in results. The number of abrasion cycles per abrasion period and abrasive wheel was set to 5000 cycles, because this number of cycles had a high wear rate but did not require resurfacing the abrasive wheels an excessive number of times.

At the end of the abrasion period the turntable is removed from the Taber instrument and placed on the measurement platform. Measurements of the wear depth are recorded and, depending on the criteria being used for replacing the abrasive wheels (either the wear criterion or the cycle criterion) during a particular test, the abrasive wheels are either left on the instrument or replaced with resurfaced abrasive wheels, and the abrasion test is continued. The test procedure is repeated for a minimum of 30,000 turntable revolutions for all specimens.

For the wet condition tests, the procedure remains the same except the vacuum nozzles are disconnected and distilled water is added to completely submerge the cable specimens. The distilled water is added to the wet-test turntable immediately before placing the abrasive wheels in contact with the test specimens. The wet test turntable accepts the same size of test specimens and uses a specimen retaining ring to securely hold the specimens, but has an additional feature compared to the dry-test turntables: a lip, or wall, along the outside edge of the turntable that makes a water-tight connection to the rubber seal placed under the specimen retaining ring. After every 5000 turntable cycles, the distilled water is removed from the turntable and replaced with clean distilled water before restarting the test. The abrasive wheels are replaced with resurfaced wheels, using the cycle criterion, after every 5000 turntable cycles for all wet condition wear tests.

Abrasive wheel resurfacing

The abrasive wheels are resurfaced after each use on the Taber Abraser instrument. The resurfacing procedure consists of mounting the pair of abrasive wheels on a mandrel which is inserted into the chuck of a lathe. Then the HDPE buildup, along with a layer of the abrasive wheels, is removed using a diamond-tipped facing tool. A thin layer of material is removed by slowly moving the facing tool back and forth across the surfaces of the rotating abrasive wheels until the tool is no longer dressing, or removing material from, the abrasive wheels. Successive thin layers of material are removed from the abrasive wheels until a uniform coloring of the working surfaces is observed visually. According to the Taber Abraser manufacturer [21], this uniform coloring indicates that the abrasive wheel working surfaces have been completely renewed. Generally during the abrasive wheel resurfacing procedure, the total thickness of material removed is approximately 0.010in.–0.015in. The diameter of each abrasive wheel is recorded before and after each refacing procedure.

Calculations

Effective coefficient of friction

The coefficient of kinetic, or sliding, friction, μ_K, is defined as the ratio of the force, F_K, required to maintain an object's constant sliding velocity divided by the normal force, G, applied by that object to the surface on which it is moving [22]. Symbolically, this relation is expressed as

$$\mu_K = \frac{F_K}{G} \quad .$$

The stopping weight produces a tension in the line, which is wrapped around the retaining nut as shown in Figure 6; therefore a moment balance is used on the abrasive wheel to find the force, equivalent to F_K, at the contact between the abrasive wheel and the turntable specimen. When the moments are summed to zero about the center of the abrasive wheel, and the equation is rearranged,

$$F_K D = W d \quad ,$$

where W is the weight of the free-hanging mass in grams, d is the diameter of the abrasive wheel retaining nut, and D is the diameter of the abrasive wheel as shown in Figure 6. After rearranging and solving for F_K,

$$F_K = \frac{W d}{D} \quad .$$

Because the combination of kinetic and static friction leads to the use of an effective coefficient of kinetic friction, the coefficient of friction μ_K is replaced by μ_E. Then μ_E is calculated according to

$$\mu_E = \frac{W d}{D N} \quad ,$$

where G has been substituted with N because N is the normal force applied by the abrasive wheel to the turntable specimen. The value of N was verified, using a spring scale, as either 250g for the 250g tests or as 500g for the 500g tests.

Abrasive energy density

Abrasive energy density is defined for this thesis as the energy expended per unit volume of material removed, and is used to evaluate the abrasion resistance of the material to a specific abrasive. The abrasive energy density is normalized to the stress at the beginning and end of each abrasion period by multiplying the abrasive energy density by the ratio of the wear areas at the beginning and end of each abrasion period.

The abrasive energy density, when normalized to stress, attempts to correct for the high stress levels at the beginning of the abrasion period. The high stresses are due to the cylindrical shape of the cables. Initially, a small area of contact occurs between the abrasive wheels and the cables (because the axes of the cyclindrical wheels and cables are not parallel). This area of contact grows as the abrasion test continues and material is abraded from the cables. Also, at the beginning of each abrasion test, the abrasive wheels travel from the high point of one cable and then "bump" onto the next cable. This bumping, and the associated high dynamic stresses, diminishes as the abrasion continues and the cables flatten due to the loss of the abraded material. Results of the calculated abrasive energy density are plotted before and after the energy density is normalized to stress, i.e., readings are corrected to a constant stress.

Let Π represent the abrasive energy density, E the expended energy, and V the volume, then

$$\Pi = \frac{E}{V} \ .$$

The abrasive energy is the amount of energy required to do the work of abrasion. The work, or energy, of abrasion, neglecting energy losses such as in the form of heat, is the frictional force times the sliding or abrasive distance. The sliding distance, S, is calculated by multiplying the radius, R, to the center of the wear path (as shown in Figure 5) by the number of turntable revolutions, n; this result is then multiplied by a factor of two because there are two abrasive wheels.

$$S = 2 \times 2\pi R n = 4\pi R n \quad .$$

The total, upper limit of effective energy, E_E, for each abrasion period is the effective frictional force times the sliding distance, so that

$$E_E = 4\pi R n \mu_E N \quad ,$$

where μ_E is the effective coefficient of friction and N is the applied normal force. The lower limit for the effective energy is given by

$$E_E = (4\pi R n \mu_E N) \tan\theta \quad ,$$

where θ is the angle between f_S and F_L as shown in Figure 5.

The volume of abraded material at each abrasion location, v_i, is a function of the wear depth and the length of the wear region at the particular abrasion location and is calculated by the equation (derived in Appendix A)

$$v_i = L_i \left[r^2 \cos^{-1}\left(\frac{r - h_i}{r}\right) - (r - h_i)\sqrt{2rh_i - h_i^2} \right] ,$$

where L_i is the length of wear region for each abrasion location, r is the cable radius, and h_i is the wear depth at each abrasion location. The total volume, V, of abraded material for all abrasion locations on the cable raft is found by summing the individual volumes of the abrasion locations;

$$V = \sum_{i=1}^{12} v_i \quad .$$

The abrasive energy density, Π, when normalized to constant stress and using the upper limit for energy, becomes

$$\Pi_\sigma = \frac{A_i}{A_f} \left[\frac{4 \pi R \mu_E N n}{V} \right] \quad ,$$

where Π_σ is the stress-normalized energy density, A_i is the initial wear area for each abrasion cycle, and A_f is the final wear area for each abrasion cycle.

Chapter 4

RESULTS

Hardness Measurements

The results from the maximum-reading Shore Type 'D' durometer were obtained from a random sampling of the sheet specimens and from cable specimens that had been cut originally from a single length of cable supplied for these tests. Each reported value is the mean of five individual, maximum value readings, in accordance with ASTM D2240–91 standards. The tests were conducted on unabraded areas of the cable and sheet specimens. The results obtained from the hardness tests are summarized in Table 2.

The cable jacket thickness is less than the thickness specified in the ASTM standard; thus values are reported for the single cable jacket and for the jacket with one and two extra layers of cable jacket added. The extra layers were obtained from a different location on the same cable by removing pieces of the cable jacket. Using a nylon line technique that was developed to cut the cable jacket without cutting the underlying steel shielding, pieces of the cable jacket (approximately 1 inch squares) were cut and then carefully pried away from the steel shielding underneath. These pieces of jacket were then laid onto an unaltered piece of cable to form double and triple layers of cable jacket.

Results of the hardness tests on the abraded cables are not reported since it was evident from the test results that the underlying steel shielding was greatly influencing the test results (hardness values were off the scale for the durometer).

Table 2. Hardness Test Results*

Material	Mean	Std. Dev.
Single Layer Cable Jacket	64.2	1.1
Double Layer Cable Jacket	64.4	0.6
Triple Layer Cable Jacket	62.4	1.1
HDPE Flat Sheet	71.4	0.6

* Shore D durometer, ser. no. 97988, with sharp (0.004in. tip radius) 30° included angle indenter.

Effective Coefficients of Friction

The mean values and standard deviations calculated for typical cable specimens are listed in Table 3. The values are for abraded cable specimens that have been subjected to 50,000 turntable cycles. Resurfaced wheels are represented as "new" and wheels that have a buildup of HDPE are represented as "full." A comparison between the frictional coefficients presented in this thesis and results presented elsewhere is made in the discussion on frictional coefficients later in this thesis.

Table 3. Effective Coefficients of Friction for Abraded Cable Specimens

Wheel	Dry Tests		Wet Tests	
	Mean	Std. Dev.	Mean	Std. Dev.
H-18 New	0.37	0.03	0.33	0.03
H-18 Full	0.32	0.02	0.28	0.02
H-22 New	0.32	0.01	a	a
H-22 Full	0.29	0.02	a	a

[a] not measured

Table 4 lists the effective coefficients of friction, μ_E, for the H-22 wheels and the flat sheets of HDPE. The "smooth sheet" represents a clean, unabraded surface and the "abraded sheet" is the surface obtained after 30,000 cycles. It is interesting to note that the μ_E for the smooth, unabraded sheet is lower than that for the abraded sheet. Since only new wheels are used on new surfaces, μ_E is not calculated for used, or full, wheels on new surfaces.

Table 4. Effective Coefficients of Friction for Flat Sheet Specimens

Wheel	Smooth Sheets		Abraded Sheets	
	Mean	Std. Dev.	Mean	Std. Dev.
H-22 New	0.37	0.03	0.33	0.04
H-22 Full	a	a	0.28	0.02

[a] not measured

Wear Depth

The following data represent the typical results obtained from the abrasion tests that were conducted. Figure 8 compares the cumulative wear depth as a

function of the number of turntable cycles for H-18 180-grit and H-22 80-grit abrasive wheels. The abrasive wheels were changed according to the wear criterion. Note that the wear depth is not proportional to the number of abrasion cycles. The lack of proportionality is due to periods (a few thousand cycles) of high wear rates followed by periods of a lower wear rate. This high-low wear rate cycle corresponds to the changing of the abrasive wheels with resurfaced wheels (when using the wear criterion, the abrasive wheels are resurfaced when the wear depth is less than 0.001in. between successive wear depth measurements). Some of the points at which the abrasive wheels were resurfaced are shown in Figure 9.
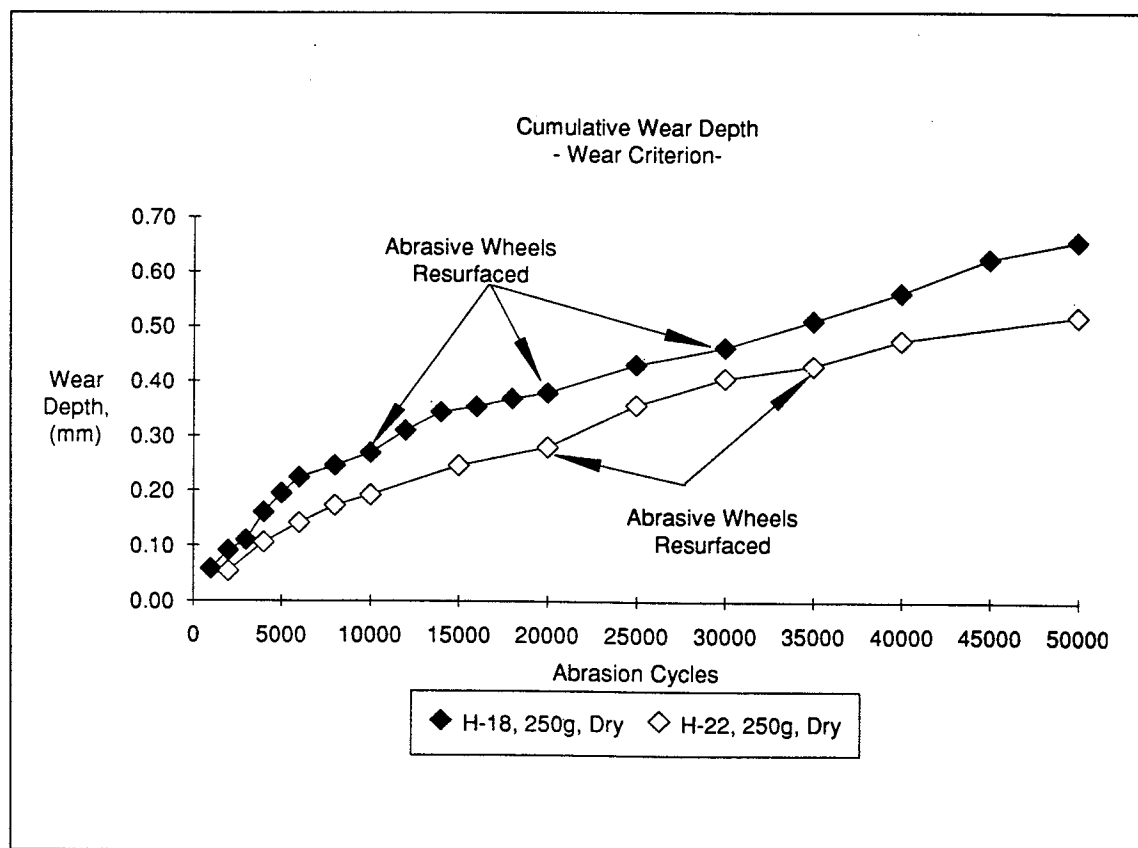
Figure 9. Cable wear depths using H-22 and H-18 wheels and the wear criterion for changing the abrasive wheels.

Figure 10 is a plot of the wear rates, for each increment of 5000 abrasion cycles, when only one set of abrasive wheels is used and the abrasive wheels are not resurfaced between abrasion periods (5000 cycles). The purpose of this plot is to see how the buildup of HDPE on the abrasive wheels affects the wear rates. The data were obtained by using a single set of H-18 abrasive wheels for the entire test. The test began with the abrasive wheels in new, resurfaced, condition and continued until the wheels were entirely filled with abraded particles of HDPE. The cables used in this test had been previously abraded for 50,000 cycles. The values shown are the average wear rates that occurred during each period of 5,000 turntable cycles. Note the decrease in wear rate after the first 5,000 cycle period. This decrease is significant because, when the abrasive wheels are used for more than 5000 cycles, the abrasive wear rate
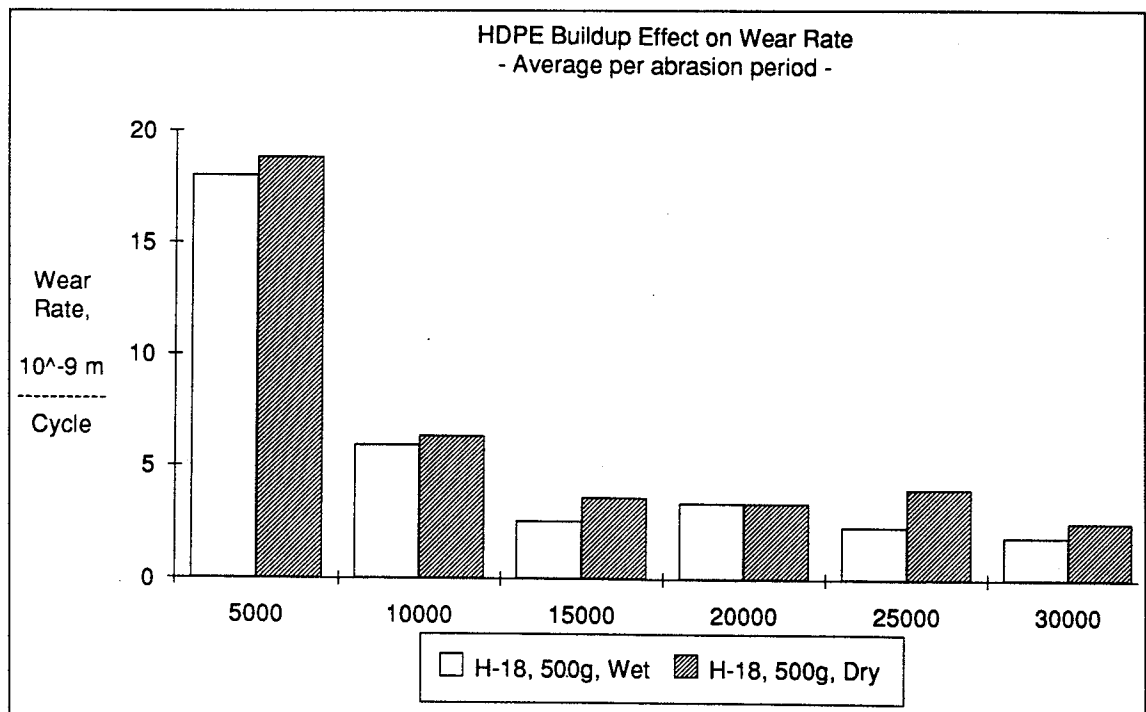
Figure 10. Wear rates for a single set of H-18 wheels, averaged every 5000 cycles, on abraded cable surfaces for dry and wet test conditions.

changes, not due to any change in or material property of the cable jacket but solely due to a change that occurs in the abrasive wheel; the abrasive wheel becomes filled with HDPE and the wear mechanism changes from an abrasive to a more adhesive mechanism of an HDPE surface on an HDPE surface.

Figure 11 shows the cumulative wear depths for H-18, 180 grit abrasive wheels with 250g and 500g loads under dry test conditions and for H-18 wheels with a 500g load under wet test conditions. For comparison, Figure 11 also
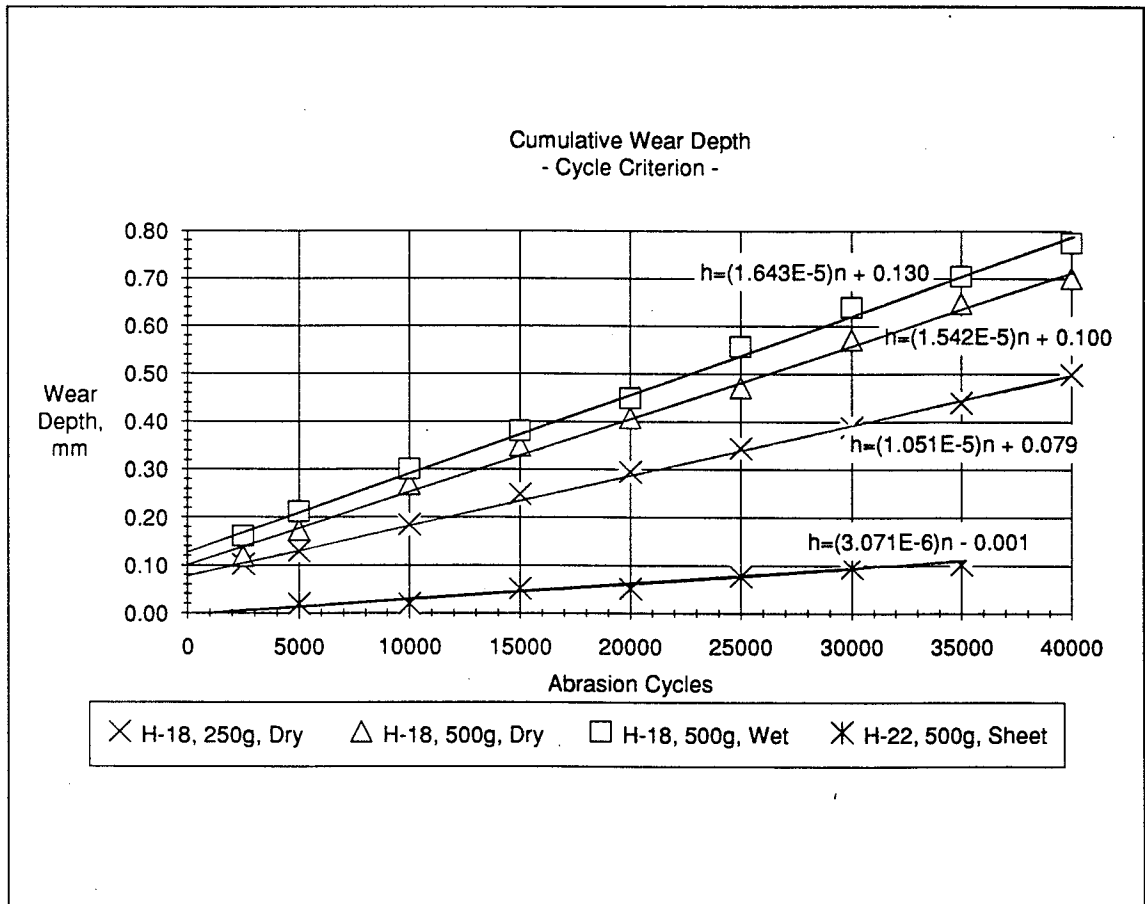
Figure 11. Cumulative cable wear depth versus number of cycles for abrasive wheels replaced every 5000 turntable cycles (cycle criterion).

shows the cumulative wear of a HDPE flat sheet specimen abraded with H-22, 80-grit wheels with 500g load. These results are compared with the cable specimens because the greatest wear depths and wear rates experienced for the sheet specimens were produced by the H-22 wheels, and the greatest wear depths and wear rates experienced for the cable specimens were produced by the H-18 wheels. The abrasive wheels were replaced, using the cycle criterion, after every 5000 turntable cycles. The wear depth for the cable specimens appears to be proportional to the number of abrasion cycles after the first 2500 cycles, and the wear depth for the flat sheet specimen appears to be proportional to the number of abrasion cycles for the entire test. The equations shown, giving the slope and wear-depth axis intercept, were obtained through linear-regression analysis of the data shown.

Figure 12 shows the cable wear rates associated with the H-18 wheels and the wear depth data shown in Figure 11. The H-18 wheels were replaced using the cycle criterion; i.e., after every 5000 turntable cycles the abrasive wheels were replaced with newly resurfaced abrasive wheels. It appears that a "steady-state" wear rate is reached after the initial abrasion period of 2500 cycles. The second abrasion period shown is also a 2500 cycle abrasion period, and the following seven abrasion periods are for 5000 cycles each. Following the first 2500 cycle abrasion period, the average wear rates for each period appear to indicate that the wear rates for all of the specimens approach a steady-state rate. The average steady-state wear rates are shown in Figure 12 as horizontal lines and represent the averages of the values shown by the columns. The columns represent the average wear rates for each abrasion period. The average steady-state
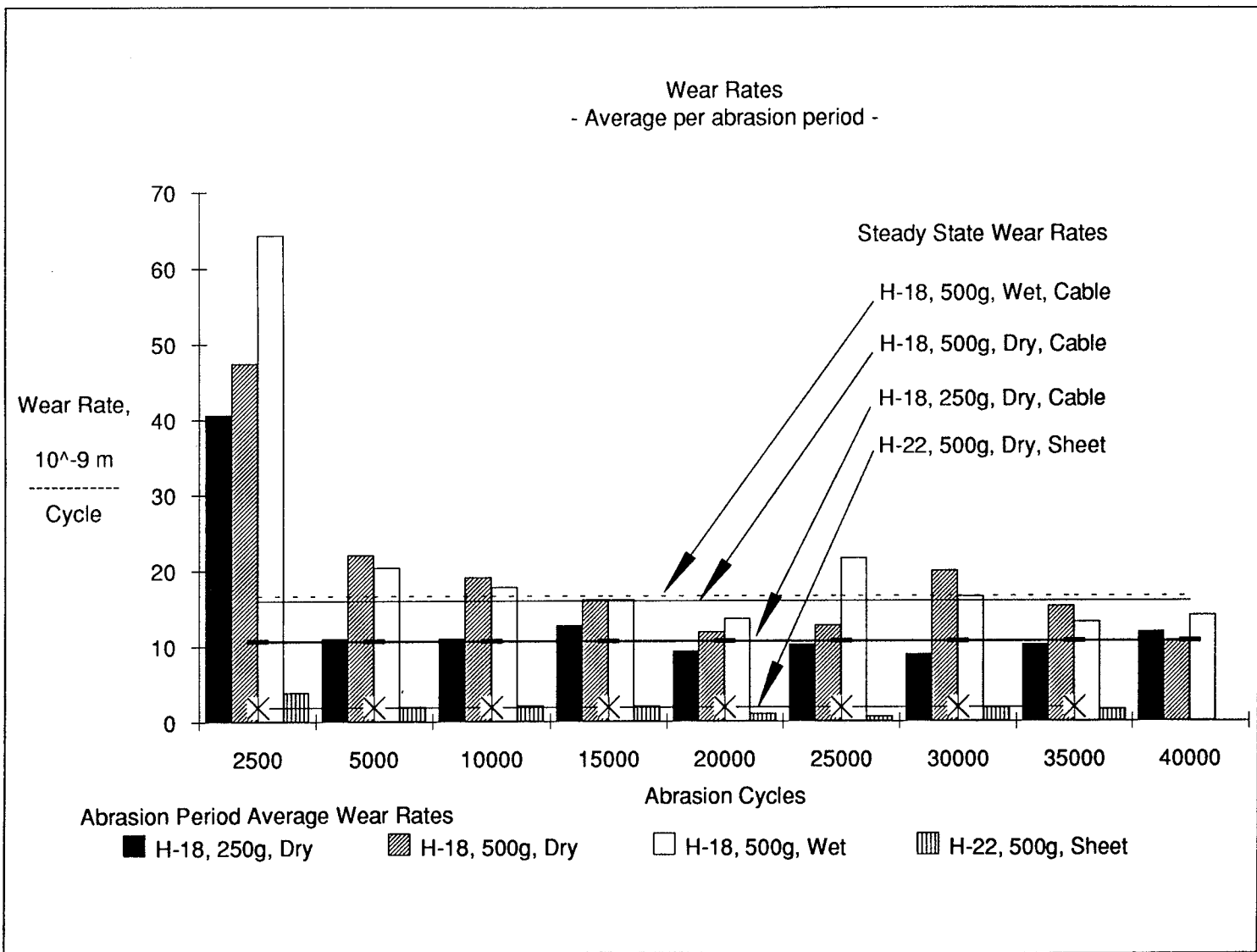
Figure 12. Average wear rates for abrasive wheels replaced, using the cycle criterion, every 5000 cycles.

wear rates (lines) do not include the values for the wear rates that occurred during the first abrasion period (2500 cycles). The initial high wear rates shown in Figure 12 explain why the cumulative wear depths, as shown in Figure 11, do not intersect the origin of the plot in Figure 11, although it is essential that the wear depths actually do intersect the origin.

Figure 12 shows that the wear rates become steady-state wear rates only after an initial number of abrasion cycles during which a transient, higher wear rate exists. The steady-state wear rates are shown as the lines in Figure 12. Figure 12 also shows that the initial period of a transient wear rate, while existing for both the cable and sheet specimens, appears to be intensified, or exaggerated, for the cable specimens. The transient and steady-state wear rates of the cable specimens are an order of magnitude greater than the wear rates of the flat sheets. The transient wear rate for the flat sheet specimen is insignificant in the overall wear of the flat sheet, while the transient rates for the cable specimens are significant in the overall wear depth of the cable specimens.

Abrasive Energy Density

The next plot, Figure 13, is a plot of the experimental abrasive energy density as a function of the number of turntable cycles. Figure 14 plots the experimental abrasive energy density normalized to the initial and final abrasion period stresses by multiplying the abrasive energy density by the ratio of the initial area to the final area of each abrasion period, also as a function of the number of

turntable cycles. Both plots (Figure 13 and Figure 14) are based on the experimental abrasive energy density that is calculated from measured cable wear depths. The energy densities for H-18 wheels and 500g loads are shown for dry and wet conditions; for comparison, the energy densities are also shown for the H-18 wheels with 250g loads and the H-22 wheels with 500g loads, both for dry condition tests.
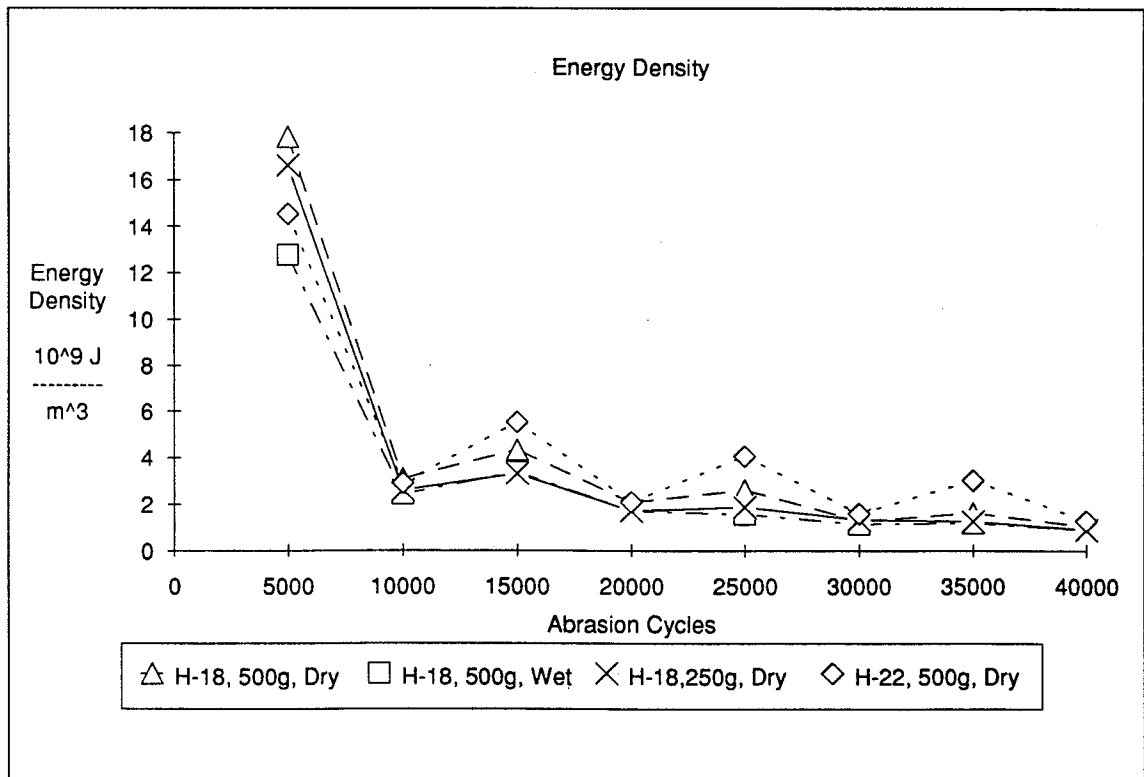
Figure 13. Abrasive energy density, for each 5000 cycle period, versus the number of abrasion cycles.
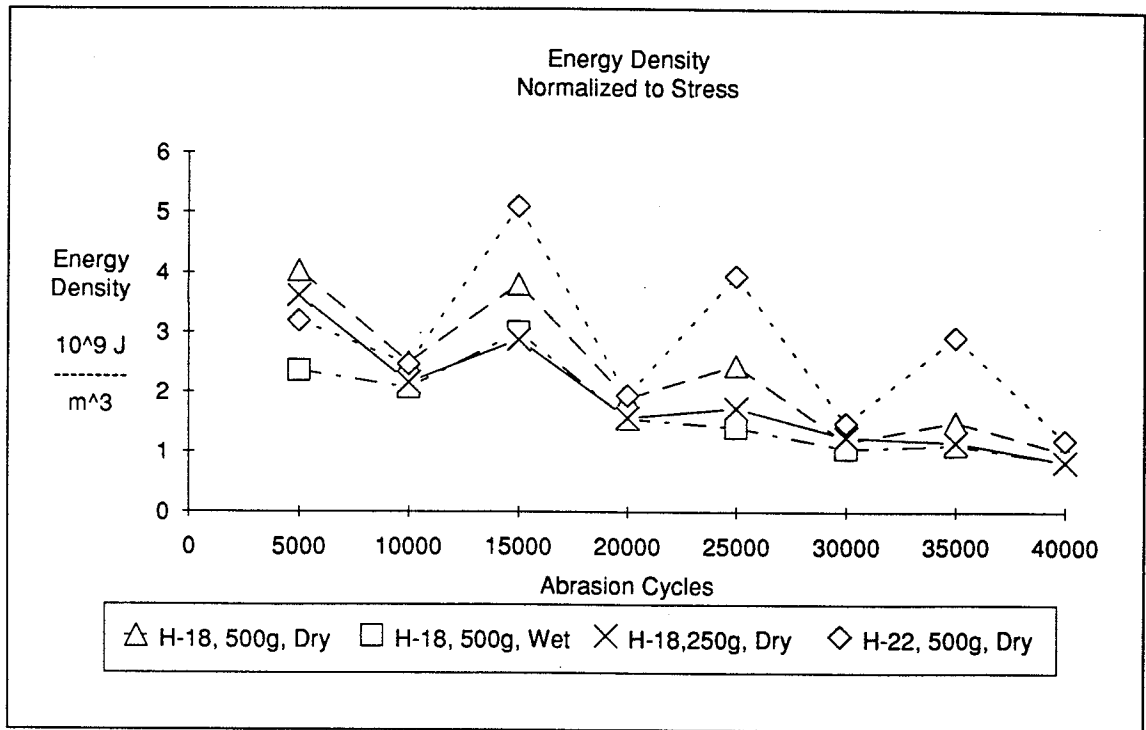
Figure 14. Abrasive energy density, normalized to stress for each abrasion period, versus the number of abrasion cycles.

Chapter 5

DISCUSSION

Specimen Hardness and Geometry

Of all the tests conducted, the greatest differences in results were obtained from the tests between the flat sheet and the cable specimens. The flat sheet had the highest hardness value and the lowest steady-state wear rate. The cable specimens had the lowest hardness value and the highest steady-state wear rates and, additionally, exhibited an initial transient wear rate, with the wet condition tests having the highest transient rate. The flat sheet's slightly higher measured hardness value of 71.4 (versus 62.4–64.4 for the cable) gave it the greatest resistance to wear and a total wear depth (at 30,000 cycles) of about 0.1mm compared to about 0.55mm for the cable specimens under the same test conditions and at the same number of turntable cycles. The flat sheet specifications, provided by Boedeker Plastics, Inc., state the sheet material's hardness as Shore D 69.

Effective Coefficients of Friction

The effective coefficients of friction for the cable and sheet specimens are consistent with published values. Deanin and Patel [14] reported coefficients of friction for several polyethylenes. For comparison, they report a range in coefficients of friction, for plastic on plastic, of 0.32–0.48 static and 0.20–0.4 kinetic, for polyethylenes with a density of 0.960 g/cc, each, and Shore D hardness of 64–68, respectively. The also list two polyethylene formulations of

"high" density with Shore D hardness values of 67 and 69, with both having a plastic on plastic coefficient of static friction of 0.32 and coefficients of kinetic friction of 0.26 and 0.24, respectively. Yamaguchi [12] reported frictional coefficients of polyethylenes in the ranges of 0.1–0.35 static and 0.14–0.25 kinetic for plastic on plastic and 0.12–0.3 kinetic for steel on plastic. Deanin's and Patel's measurements agree very well with the coefficients determined in this thesis even though their measurements were made for plastic on plastic. Some of the effective coefficients of friction in this thesis are slightly higher than the frictional coefficients cited by Yamaguchi. His frictional coefficients were evaluated for plastic on plastic or steel on plastic, both of which are very different material combinations. However, the effective coefficients of friction presented in this thesis are found to be similar to the expected values for polyethylene as presented in the literature. The observation is made that these effective coefficients of friction are within reasonable engineering tolerances, but that these effective coefficients of friction are based on the assumptions stated earlier in this thesis.

The frictional coefficients, as shown in Table 3, decreased from the initial value for the unabraded surfaces to a lower value for the abraded surfaces. This result was also expected because the abraded surface has semi-loose particles, or particles that are partially torn away from the bulk material which the abrasion wheel is contacting. The semi-loose particles require less energy to be sheared and removed from the bulk material than the energy required to initially create the particles from the unabraded surfaces. In essence,

the semi-loose particles allow for easier movement to occur between the abrasive wheel and the bulk specimens.

Wear Criterion Versus Cycle Criterion

Wear depth as a function of the number of turntable revolutions, or cycles, is not a complete, directly proportional relation when the wear criterion is used as a basis for resurfacing the abrasive wheels, or if the abrasive wheels are not resurfaced. The wear rate is greatest initially and slowly decreases. Close examination of the wear depth plotted in Figure 9 reveals what appears to be a proportional relation in localized regions (generally toward the latter cycles of the test). In fact, closer examination of the data reveals that these regions resulted when the abrasive wheels were changed after consistent numbers of turntable revolutions. At least a very general trend was noticed, and so the effects of the polyethylene loading on the abrasive wheel, and the subsequent effects on the wear rate, was further investigated.

In Figure 10 the buildup of an HDPE layer, or coating, onto the abrasive wheels causes the wear rates to decrease. The wear rate drops in the second period to ¼ the wear rate in the first period. By the end of the test, there is almost an order of magnitude difference in the wear rates between the first and last abrasion periods. The differences in the effective coefficients of friction between new wheels and used wheels probably does not entirely account for the difference in wear rates between the first period and last period in Figure 10.

Instead, the difference in wear rates likely results from the abraded HDPE particles filling in-between and around the wheel's abrasive particles, which creates a coating, or layer, of HDPE on the abrasive wheels. The HDPE buildup, filling, and covering that occur on the abrasive wheels reduce the amount of material that can be removed by reducing the amount of bite the individual abrasive particles, or cutting teeth, can make in the substrate.

When the abrasive wheels are resurfaced, using the cycle criterion, a proportional relation develops between wear depth and number of turntable cycles. In Figure 11, the wear depth is almost a straight line that is proportional to the number of turntable cycles, after the initial abrasion period. The lines in Figure 11, which are fit to the data using a linear-regression analysis, do not intersect the origin of the plot. This was not expected because similar abrasion data obtained by Yamaguchi [12], using a Tabor Abraser, H-22 abrasive wheels, and 1000g load, showed a highly proportional relation between wear volume and sliding distance (and number of turntable revolutions) with lines of proportionality intersecting the plot's origin. The only specimens used in Yamaguchi's tests were flat sheet plastic materials. However, the only data presented in Yamaguchi's report were for a maximum of 5000 turntable revolutions (cycles) and the number of, or criterion used for, abrasive wheel resurfacings was not stated.

The line for the flat sheet wear data also does not intersect with the plot origin; however, it does come much closer (within 0.001mm) than the data line for the closest cable specimen (0.08mm). Also, the linear regression gives a negative value for the flat sheet data's intercept point on the wear-depth axis, and the

data line must actually intercept at the origin. It is most likely due to experimental error that it doesn't. The accuracy of the depth measurements (±0.0005in. or ±0.013mm) does account for the slight discrepancy in the flat sheet data, but does not account for the cable data lines not intersecting the plot origin.

Transient Versus Steady-State Wear Rates

In addition to not intersecting the origin of the wear depth data plots, Figure 12 illustrates that there is an initial period of a high wear rate, or transient wear rate, followed by a more consistent, or "steady-state," wear rate. An initial transient rate is seen in Figure 12 for both the cable and flat sheet specimens, although the cable specimens exhibit a much greater, or higher, transient (roughly an order of magnitude greater) than the flat sheet specimens. Yamaguchi [12] reported a similar, initially higher transient wear rate followed by a steady-state wear rate in his investigations of the adhesive wear behavior of polycarbonate and Nylon 6 sheet materials. However, his results for the abrasive wear behavior of polymeric sheet materials showed a direct proportional relationship, without an initial transient rate, between wear volume and sliding distance (turntable cycles).

The high transient wear rates reported in this thesis occurred only during the wear of the cable specimens. During the wear of the HDPE sheeting, the wear rates and wear volumes were more consistent with the flat sheet results pre-

sented by Yamaguchi. The presence of the high transient wear rate during the wear of the cable specimens is believed to be caused, at least in part, by the cylindrical cable shape, because if the cable jackets were flat instead round the relation between wear depth and turntable cycles would be expected to be directly proportional. Other likely causes of the high transient wear rate are the surface energy of unabraded surfaces compared to abraded surfaces, and the difference in surface texture between smooth unabraded surfaces and rough abraded surfaces, where the unabraded surfaces require more energy for wear rates to be similar to the wear rates of abraded surfaces.

Wet Versus Dry Test Conditions

In both Figure 11 and Figure 12, the results obtained for the wet and dry test conditions are strikingly similar. The effective coefficients of friction are less for the abrasive wheels on the wet cable, but the cumulative wear depth shown in Figure 11 is greater for the wet cables than for the dry cables. The steady-state wear rates are roughly equivalent (difference of 0.101×10^{-5}mm/cycle, or 0.04mm after 40,000 cycles), yet the total depth is greater for the wet cables. The difference is attributable to the difference in initial transient wear rates, which are evidenced by the difference in wear-depth axis intercepts (difference between wet and dry conditions of 0.03mm). The wet test conditions have a greater transient rate than the dry condition tests. The steady-state wear rate difference is small but, when combined with the transient rate difference, causes

the overall depth to be greater for the wet tests. However, after 40,000 cycles, the total difference in wear depth between the wet and dry test conditions is less than 0.1mm. The slightly higher steady-state wear rates, during the wet condition tests, may also be due to localized cooling of the HDPE and prevention of HDPE buildup on the abrasive wheels.

Abrasive Energy Density

The existence of the initial high energy density is due to the cable shape, or geometry. Initially, the cable shape limits the area of contact between the cable surface and the abrasive wheels. The small contact area causes an increase in stress and an increase in wear rate (depth per cycle) to occur. Initially, although the wear rate is high, the wear area and volume are small. Because the energy remains constant, the small abraded volume causes the energy density to be very large. In addition to the limits imposed by the cable shape on the wear area at the beginning of the test, there is another factor that explains the large energy density and small abraded volume that occurs at the beginning of the tests: surface energy.

When the wear process is beginning, the abrasive wheels are creating entirely new surfaces from the unabraded cable surfaces. As the wear depth increases, the amount of abraded surface in contact with the abrasive wheels versus the amount of unabraded surface increases. A greater amount of energy is required to create a newly abraded surface from an unabraded surface than the amount

of energy required to abrade a previously abraded surface. The effects of the abraded versus unabraded surface were also seen in the effective coefficient of friction, which decreased from the unabraded surface value to the abraded surface value. Thus initially more energy is used to create the abraded surface from the unabraded surface. As the test period progresses, the energy expended transfers from creating an abraded surface out of an existing smooth surface to removing the loose, abraded material.

Chapter 6

CONCLUSIONS

1. A Taber Abraser with a turntable platform modified for small diameter cables and conventional abrasive wheels can measure the relative abrasion resistance of the cable jacket. The advantages of using the Taber Abraser are that the actual cable can be used as test specimens and the test period is approximately 18 hours for the 0.762mm (0.030in.) nominal cable jacket thickness. Thus the final, production-line product can be evaluated and compared, within a reasonable time period, with standards, specifications, and other cable production samples or specimens.

2. The HDPE flat sheet specimens (with a hardness of 71 Shore D) abrade much more slowly—about six times more slowly—than the HDPE cable jacket specimens (hardness of 64) after the initial wear of the cable produces a flat surface. The dynamics of the abrasive wheels while "bumping" over the cables may increase the wear rates. The continuous availability, to the abrasive wheels, of surface (wear area) edges on the cable specimens are suspected to also enhance wear rates. Observation of the wear action and wear patterns shows that one wheel scrubs (wears) outwardly and one wheel scrubs (wears) inwardly, causing a reciprocating wear action of the abrasive wheels at each wear area, or location, on the test specimens. However, the presence of unknown fillers in the HDPE flat sheet material may have also contributed to the observed lower wear rates compared to the cable specimens.

3. Test results show that two H-18 wheels, when resurfaced every 5,000 turntable cycles, will produce a nearly linear, or proportional, wear depth rate to a nominal depth of 0.71mm (0.028in.) under dry test conditions and

0.76mm (0.030in.) under wet test conditions in 40,000 turntable cycles and 500g normal load. Tests results also show that two H-22 wheels, when resurfaced every 5,000 turntable cycles, will produce a nearly linear, or proportional, wear depth rate to a nominal depth of 0.50mm (0.020in.) under dry test conditions in 40,000 turntable cycles and 500g load.

4. Interestingly, the H-18 180-grit abrasive wheels tend to wear the cable specimens faster than the H-22 80-grit abrasive wheels. The finer H-18 wheels (180-grit) have a greater number of cutting edges than the coarser H-22 wheels (80-grit). However, as was expected, higher applied normal forces (or loads) caused higher wear rates for both types of abrasive wheels and both test conditions (dry and wet). Doubling the normal force did not produce twice the wear rate, however, which implies that wear would still occur if the normal force, or load, approached zero (but the abrasive wheels remained in contact with the specimens).

5. Ideally, wear rates would be evaluated for a given wheel HDPE buildup (coating) condition, i.e., changing the wheels when the HDPE buildup reduces wear depth to less than 0.025mm (0.001in.) per given number of turntable cycles. In order to standardize the test procedures, the cycle criterion was developed where the abrasive wheels were resurfaced after a set number of cycles, i.e., 5,000 cycles; the wear depths obtained afterwards became proportional to the number of cycles, and the test results of the same test conditions became more consistent and repeatable.

6. Buildup of HDPE on the abrasive wheels tends to decrease the wear rate as the wheels begin to be filled and coated. The HDPE coating of the abrasive wheels causes the wear mechanism to transform from predominantly abrasive cutting to adhesive sliding wear. The latter wear rate tends to be much slower (an order of magnitude) than the former. Regular resurfacing of the abrasive wheels reduced the effects of the decreasing wear rate caused by the filling and coating of the abrasive wheels. The difference between resurfaced abrasive wheels (μ_E = 0.32–0.37) and full, used abrasive wheels (μ_E = 0.29–0.32) does not account for the difference in wear rates.

7. Initial results of the wet test conditions indicate that the wet abrasive wear rates tend to be higher than the dry abrasive wear rates during the initial transient wear rate period and roughly equivalent during the steady-state wear rate period. The enhanced wear rates of the wet condition tests may be due to localized cooling of the HDPE and prevention of HDPE buildup on the abrasive wheels.

8. The initial results of the energy density calculations provide an upper bound on the energy density required to produce a specific wear rate. The energy density was shown to asymptotically approach a steady-state value. This steady-state value of the experimental energy density is of the right order of magnitude that would be expected for HDPE when compared to theoretical approximations of the toughness of HDPE. Although not conclusive at this time, the evidence suggests that energy density and toughness should be further investigated relative to abrasion and wear resistance.

9. Through the use of the proper test procedures, the Taber Abraser is capable of evaluating the wear resistance of submarine cable jackets. As a comparison test method, the Taber Abraser can provide reliable and reproducible results on the wear behavior of different HDPE formulations used for cable jackets. Either the H-18 or H-22 abrasive wheels can be used as long as the test results to be compared are the test results from the same abrasive wheel type, that is, compare the results from H-18 wheels to results from H-18 wheels, or compare the results from H-22 wheels to results from H-22 wheels.

Chapter 7

FURTHER RECOMMENDATIONS

This thesis has answered many of the questions that arose from the previous study on the use of the Taber Abraser as a test method to evaluate the wear behavior of submarine cable jackets. However, the current thesis has also raised some new questions that should be addressed in future investigations. To begin with, some of the new questions to address, or tests to perform, are

- What effect will seawater have on the wear behavior?

- What effect will high hydrostatic pressure have on the wear behavior?

- Will the wear behavior during wear tests on cylinders that are cut from sheet material be the same as the behavior that was observed during the tests on the extruded cable jacket?

- Can a simple, quick test method be developed to evaluate both static and kinetic friction between the abrasive medium and the actual cable jacket for both parallel with and perpendicular to the cylinder axis?

- Can the hardness of the jacket material be used as an indicator of the relative wear resistance? Probably not alone, but maybe in combination with surface energy or through the combination of ductility and tensile strength (toughness), a wear-resistance indicator can be found.

- Preliminary comparisons of the steady-state region of the calculated energy density to the theoretical toughness values of HDPE show that the two values are within an order of magnitude. Can measured toughness values of the HDPE be an indicator of the material's resistance to abrasion? Is the following equation true?

$$\frac{E}{V} = \sigma \, \varepsilon = \text{Toughness ?}$$

  Or is it a useful approximation, where σ is true stress and ε is true strain?

Some of these questions can be answered with a simple experiment, while some of the questions may be answered only after a lengthy series of tests. However, with the growing number of submarine cable applications and subsequent cable deployments, these questions should be answered.

LIST OF REFERENCES

[1]   Chave, A. D., Butler, R., and Pyle, T. E., "Submarine telephone cable technology," Workshop On Scientific Uses of Undersea Cables, Joint Oceanographic Institute, Inc., August 1990.

[2]   Jones, S. R., "The protection and installation of submarine cable in hazardous deep water areas," Submarine Telecommunications Systems, IEEE Conf. Pub. No. 183, New York, February 1980, pp. 77

[3]   Gerlock, John L., and Bauer, David R., "Photolytic degradation," *Engineering Materials Handbook,* Vol. 2, ASM International, Metals Park, Ohio, 1988, pp. 776–782.

[4]   Bowden, F. P., and Tabor, D., *The Friction and Lubrication of Solids*, Oxford University Press, New York, 1964.

[5]   Rabinowicz, E., *Friction and Wear of Materials*, John Wiley and Sons, Inc., New York, 1965.

[6]   Bartenev, G. M. and Lavrentev, V. V., *Friction and Wear of Polymers*, Lee, L.h., and Ludema, K.C., ed., Elsevier Science Publishing Co., Netherlands, 1981.

[7]   Naval Civil Engineering Laboratory, "Abrasion testing of cables in suspension," NCEL Techdata Sheet 92–04, NCEL, Port Hueneme, CA, March 1992.

[8]   Sandwith, C. J., and Ruedisueli, R. L., "Corrosion testing of the steel shield of a small deep-sea electro-optic cable," Oceans '91 proceedings, vol.1, Institute of Electrical and Electronics Engineers, Inc., Honolulu, Hawaii, October 1991, pp. 301–305.

[9]   Merchant, M. E., "Friction and adhesion," *Interdisciplinary Approach to Friction and Wear*, Proceedings, National Aeronautics and Space Administration, Washington D. C., 1968, pp. 181–211.

[10]   Bikerman, J. J., "The nature of polymer friction," *Advances in Polymer Friction and Wear*, Lee, L. H., ed., Vol. 5B, Plenum Press, New York, 1974, pp. 149–163.

[11]   Archard, J. F., "Wear," *Interdisciplinary Approach to Friction and Wear*, Proceedings, National Aeronautics and Space Administration, Washington D. C., 1968, pp. 267–304

[12]   Yamaguchi, Y., *Tribology of Plastic Materials, Tribology Series*, Elsevier Science Publishers, New York, 1990, pp. 93–141.

[13]   Sandwith, C. J., and Breiwick, T., "High-velocity ice particles for cleaning ship hulls: A feasibility study," Proceedings of the 4th International Congress on Marine Corrosion and Fouling, Boulogne, France: Centre de Recherches et d'Etudes Oceanographiques, 1976, pp. 93–141.

[14]   Deanin, R. D., and Patel, L. B., "Structure, properties and wear resistance of polyethylene," *Advances in Polymer Friction and Wear, Polymer Science and Technology*, vol. 5B, Plenum Press, New York, 1974, pp. 569–580.

[15]   *personal communication*, Sandwith, C. J., University of Washington, November 1992.

[16]   Bahadur, S., and Tabor, D., "Role of fillers in the friction and wear behavior of high-density polyethylene," *Polymer Wear and Its Control*, American Chemical Society, Washington, D. C., 1985, pp. 253–266.

[17] Dowson, D., El-Hady Diab, M. M., Gillis, B. J., and Atkinson, J. R., "Influence of counterface topography on the wear of ultra high molecular weight polyethylene under wet or dry conditions," *Polymer Wear and Its Control*, Washington, D. C., American Chemical Society, 1985, pp. 171–187.

[18] Sandwith, C. J., Ruedisueli, R. L., and Welch, M. L., "A standardized abrasion resistance test for undersea cable jackets," Oceans '91 proceedings, Honolulu, Hawaii, Institute of Electrical and Electronics Engineers, Inc., October 1991, vol. 1, pp. 296–300.

[19] SPAWAR-C-833D Cable, Fiber Optic, Deep Water Trunk, Space and Naval Warfare Systems Command (PMW 184), Department of the Navy, Washington, D.C., July 26, 1990, pp. 4–18.

[20] *personal communication,* Jalufka, J., Boedeker Plastics, Inc., Shiner, Texas, June 30, 1991.

[21] *Operating Instructions for Taber Models 5130 & 5150 Digital Abrasers with LED Readouts,* Teledyne Taber, Inc., North Tonawanda, New York, 1984, pp. 42–43.

[22] Halliday, D., and Resnick, R., *Fundamentals of Physics,* 3rd ed., John Wiley and Sons, Inc., New York, 1988, pp. 117.

BIBLIOGRAPHY

Anderson, J. C., and Williamson, P. K., "Relating laboratory wear testing to the in-service wear of polymers," *Polymer Wear and Its Control*, Lee, L. H., ed., American Chemical Society, 1985.

Archard, J. F., "Wear," *Interdisciplinary Approach to Friction and Wear*, Ku, P.M., ed., NASA SP-181, Washington, D.C., 1968, pp. 267–333.

Bahadur, S., and Tabor, D., "Role of filllers in the friction and wear behavior of high-density polyethylene," *Polymer Wear and Its Control*, Lee, L. H., ed., American Chemical Society, 1985, pp. 253–268.

Bahadur, S., and Ludema, K. C., "The viscoelastic nature of the sliding friction of polyethylene, polypropylene, and copolymers," *Wear*, Vol. 18, 1971, pp. 109–128.

Bely, V. A., Sviridenok, A. I., Petrokovets, M. I., and Savkin,V. G., *Friction and Wear in Polymer-Based Materials*, Pergamon Press, 1982, pp. 33–187.

Belyi, V. A., and Nevzorov, V. V., "Molecular features of transfer fragments when high-density polyethylene rubbed against metals," *Polymer Wear and Its Control*, Lee, L. H., ed., American Chemical Society, 1985, pp. 206–212.

Blanchet, T. A., and Kennedy, F. E., Jr., "The developement of transfer films in ultra-high molecular weight polyethylene/stainless steel oscillatory sliding," *Tribology Transactions*, Vol. 32, No. 3, 1989, pp. 371–379.

Buckley, D.H., and Aron, P.R., "Characterization and measurement of polymer wear," *Polymer Wear and Its Control*, Lee, L.H., ed., American Chemical Society, 1985, pp. 287–301.

Deanin, R.D., and Patel, L.B., "Structure, properties, and wear resistance of polyethylene," *Advances in Polymer Friction and Wear*, Lee, L.H., ed., Vol. 5B, Plenum Press, New York, 1974, pp. 569–583.

Dieter, G. E., "Polymeric materials," *Mechanical Metallurgy*, McGraw-Hill, 1976, pp. 292–325.

Dowson, D., El-Hady Diab, M. M., Gillis, B. J., and Atkinson, J. R., "Influence of counterface topography on the wear of ultra high molecular weight polyethylene under wet or dry conditions," *Polymer Wear and Its Control*, Lee, L. H., ed., American Chemical Society, 1985, pp. 171–187.

Eiss, N. S. Jr., and Potter, J. R. III, "Fatigue wear of polymers," *Polymer Wear and Its Control*, Lee, L.H., ed., American Chemical Society, 1985, pp. 59–65.

Eiss, N. S., Jr., *et al.,* "Model for the Transfer of Polymer to Rough, Hard Surfaces," *Transactions of the ASME*, Vol 101, April 1979, pp. 212–219.

Engel, L., Klingele, H., Ehrenstein, G. W., Schaper, H., *An Atlas of Polyurer Damage*, Wolfe Science Books, 1901.

Jones, S.R., "The protection and installation of submarine cable in hazardous deep water areas," *International Conference on Submarine Telecommunications Systems*, Institute of Electrical Engineers, 1979, pp. 77–81.

Kragelsky, I. V., Bely, V. A., and Sviridyonok, A. I., "Peculiarities of real contact area formation of polymers during friction interaction," *Advances in Polymer Friction and Wear*, Lee, L. H., ed., Vol. 5B, Plenum Press, New York, 1974, pp. 729–743.

Layne, A. A., ed., *Materials Engineering*, Vol. 70, No. 5, 1969, pp. 200–201.

MacGregor, C. W., ed., *Handbook of Analytical Design for Wear*, Plenum Press, New York, 1964.

Marcucci, M. A., "Friction and abrasion characteristics of plastic materials," *SPE Journal*, February 1958, pp. 30–33.

Merchant, M. E., "Friction and adhesion," *Interdisciplinary Approach to Friction and Wear*, Ku, P. M., ed., NASA SP-181, Washington, D.C., 1968, pp. 181–210.

Nielson, L. E., *Mechanical Properties of Polymers and Composites*, Marcel Dekker, Inc., New York, 1974.

Orgorkiewicz, R. M., ed., *Thermoplastics: Properties and Design*, John Wiley and Sons, Great Britain, 1974.

Powell, P. C., *Engineering With Polymers*, Chapman and Hall Ltd., New York, 1983.

Rorrer, R. A., Mabie, H. H., Eiss, N. S., Jr., and Furey, M. J., "The wear and friction of polyvinyl chloride coatings under fretting conditions," *STLE Transactions*, Vol. 31, No. 1, pp. 98–104.

Sperling, L. H., *Physical Polymer Science*, John Wiley and Sons, New York, 1986.

Tanaka, K., and Uchiyama, K., "Friction, wear and surface melting of crystalline polymers," *Advances in Polymer Friction and Wear*, Lee, L. H., ed., Vol. 5B, Plenum Press, New York, 1974, pp. 499–531.

West, G. H., and Senior, J. M., "Frictional properties of polyethylene", *Wear*, Vol. 19, 1972, pp. 37–52.

Yamaguchi, Y., *Tribology of Plastic Materials*, Elsevier Science Publishers, Netherlands, 1990, pp. 27–142.

APPENDIX A:

DATA

H-18   HDPE CABLE   4/17/92
Dry   250g Load

Cable Specimens   Depth, (x10^3 inches)

Cycles	1a	2a	3a	4a	5a	6a	6b	5b	4b	3b	2b	1b	Average
1000	3	2	2	2	2	3	2	2	2	2	2	3	2.3
2000	1	1	1	1	1	2	2	1	1	2	2	1	1.3
3000	1	1	1	1	0	1	1	0	1	0	1	1	0.8
4000	1	2	2	2	3	2	2	2	2	2	2	2	2.0
5000	1	1	1	1	1	2	1	1	2	2	1	2	1.3
6000	1	1	1	2	2	1	1	1	1	1	1	1	1.2
8000	1	1	1	0	0	1	1	1	1	1	1	1	0.8
10000	1	0	1	1	1	1	1	1	1	1	1	1	0.9
12000	2	2	1	2	2	2	1	1	1	1	2	2	1.6
14000	1	1	2	1	1	1	2	2	1	2	1	1	1.3
16000	0	0	0	0	1	1	0	1	1	0	0	1	0.4
18000	1	1	1	1	0	1	1	0	0	1	0	0	0.6
20000	0	0	0	0	1	0	0	1	1	0	1	1	0.4
25000	2	2	2	2	2	2	2	2	2	3	2	2	2.1
30000	1	1	2	2	1	1	1	1	1	1	1	2	1.3
35000	2	2	2	1	2	2	2	2	2	2	2	2	1.9
40000	2	2	2	2	2	2	2	2	2	2	2	2	2.0
45000	4	3	2	2	3	3	2	3	2	1	2	3	2.5
50000	2	1	1	1	1	1	2	1	1	2	1	2	1.3

H-18   HDPE Cable Jacket   6/18/92
Distilled Water   250 g.

Cable Specimens   Depth, (x10^3 inches)

Cycles	1a	2a	3a	4a	5a	6a	6b	5b	4b	3b	2b	1b	Average
2000	4	3	3	4	5	4	3	4	3	3	4	3	3.6
4000	2	2	2	2	2	2	2	2	2	3	2	2	2.1
6000	0	1	1	0	1	1	1	1	1	1	1	0	0.8
8000	1	1	1	1	1	1	1	0	1	1	1	1	0.9
10000	2	1	1	2	1	1	1	1	1	1	0	1	1.1
15000	1	2	2	2	3	3	2	2	2	2	3	3	2.3
20000	1	2	2	3	2	2	2	2	2	2	2	2	2.0
25000	1	1	1	1	0	1	1	1	1	2	1	1	1.0
30000	3	2	3	3	2	2	2	1	2	2	2	1	2.1
35000	0	1	0	1	0	1	1	1	1	1	1	1	0.8
40000	1	1	1	1	1	1	1	1	1	1	1	1	1.0
50000	0	3	2	6	4	2	4	3	3	4	5	3	3.3

H-18   HDPE CABLE   6/25/92
Dry   250g Load

Cable Specimens . Depth, (x10^-3)

Cycles	1a	2a	3a	4a	5a	6a	6b	5b	4b	3b	2b	1b	Average
2500	6	3	3	4	5	4	4	3	4	4	3	5	4.0
5000	0	1	2	1	1	1	2	1	1	1	1	1	1.1
10000	3	3	2	2	2	2	2	2	2	1	3	2	2.2
15000	2	2	3	3	2	2	3	3	3	3	2	2	2.5
20000	2	2	2	2	2	2	1	1	2	2	2	2	1.8
25000	1	1	2	2	2	2	2	2	2	3	3	2	2.0
30000	2	2	1	2	3	1	1	1	2	2	2	2	1.8
35000	2	2	2	1	1	2	2	3	2	2	2	3	2.0
40000	3	2	3	2	3	2	3	2	2	2	2	2	2.3

H-18   HDPE CABLE   6/25/92
Dry   500g Load

Cable Specimens   Depth, (x10^-3)

Cycles	1a	2a	3a	4a	5a	6a	6b	5b	4b	3b	2b	1b	Average
2500	4	3	4	4	5	6	5	4	5	5	5	6	4.7
5000	3	2	2	2	2	3	2	2	2	3	1	2	2.2
10000	3	3	4	5	4	3	3	4	3	4	5	4	3.8
15000	3	2	3	3	3	4	4	3	3	3	3	4	3.2
20000	2	3	3	2	2	2	2	2	3	2	2	3	2.3
25000	3	2	2	3	3	3	2	2	2	4	3	1	2.5
30000	4	3	4	4	3	4	3	4	4	4	4	6	3.9
35000	4	3	3	2	3	3	3	2	3	2	4	4	3.0
40000	2	2	2	2	2	1	4	3	1	2	2	2	2.1

H-18   HDPE CABLE   6/25/92
Wet   500g Load

Cable Specimens   Depth, (x10^3 inches)

Cycles	1a	2a	3a	4a	5a	6a	6b	5b	4b	3b	2b	1b	Average
2500	8	7	5	7	8	7	6	5	6	5	5	7	6.3
5000	2	2	2	1	0	2	3	2	2	2	3	3	2.0
10000	4	2	3	4	4	5	3	3	3	4	3	4	3.5
15000	3	3	4	3	3	3	3	4	3	3	3	3	3.2
20000	3	3	2	2	2	3	3	2	3	2	3	4	2.7
25000	5	4	4	4	4	6	4	3	4	4	3	6	4.3
30000	5	3	3	2	2	4	5	4	3	2	3	3	3.3
35000	4	3	2	3	1	1	4	3	3	4	2	1	2.6
40000	2	2	2	4	3	5	2	2	1	1	3	6	2.8

H-22   HDPE Flat Sheet   6/25/92
Dry   500g Load

Flat Sheet   Depth, (x10^3 inches)

Cycles	A	B	C	D	Average
5000	1	0	1	1	0.8
10000	0	0	0	0	0.0
15000	1	2	1	1	1.3
20000	0	0	0	0	0.0
25000	1	1	1	1	1.0
30000	1	1	0	1	0.8
35000	0	0	1	0	0.3

H-18   HDPE Flat Sheet   4/17/92
Dry   500g Load

Cycles	Flat Sheet A	B	Depth, (x10^3 inches) C	D	Average
4000	1	1	1	1	1
10000	1	1	2	1	1.25
20000	1	1	1	1	1
30000	1	1	1	1	1

H-22   HDPE Cable Jacket   6/18/92
Dry   500g Load

Cable Specimens   Depth, (x10^3 inches)

Cycles	1a	2a	3a	4a	5a	6a	6b	5b	4b	3b	2b	1b	Average
2000	3	4	4	5	4	5	5	3	4	4	5	5	4.3
4000	2	1	2	2	2	2	1	2	2	2	3	2	1.9
6000	0	1	0	0	1	1	1	0	1	0	0	0	0.4
8000	2	2	3	3	2	1	1	2	2	3	3	2	2.2
10000	1	2	1	1	2	2	2	1	1	2	2	2	1.6
15000	2	1	2	3	2	2	1	2	2	2	2	2	1.9
20000	2	2	2	2	2	2	2	2	2	2	3	1	2.0
25000	0	1	1	1	1	1	0	1	1	2	1	1	0.9
30000	2	2	2	2	2	2	2	2	2	2	2	3	2.1
35000	1	1	1	2	1	2	1	1	1	1	1	1	1.2
40000	2	2	2	1	2	2	2	2	2	2	2	2	1.9
50000	4	5	4	5	5	5	4	4	4	4	4	4	4.3

H-22   HDPE Cable Jacket   6/18/92
Dry   250g Load

Cable Specimens   Depth, (x10^3 inches)

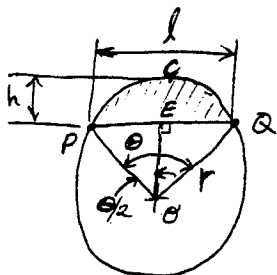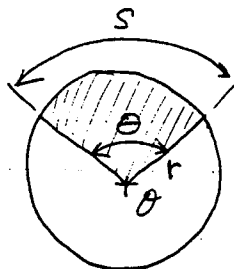| Cycles	1a	2a	3a	4a	5a	6a	6b	5b	4b	3b	2b	1b	Average
2000	2	2	2	2	2	3	2	2	2	3	1	2	2.1
4000	2	1	2	2	2	2	3	2	2	2	3	2	2.1
6000	2	1	1	2	1	1	1	1	2	2	1	2	1.4
8000	0	2	2	2	1	2	1	1	1	1	1	1	1.3
10000	1	0	0	0	1	1	1	1	1	2	0	1	0.8
15000	2	2	3	2	2	1	2	1	2	4	2	2	2.1
20000	0	1	2	2	2	1	1	1	1	3	1	1	1.3
25000	1	1	1	1	2	2	21	2	2	1	2	1	3.1
30000	2	2	2	2	2	2	2	1	2	3	1	2	1.9
35000	1	1	1	1	0	1	1	1	1	1	1	1	0.9
40000	2	2	2	2	2	1	1	2	2	2	2	2	1.8
50000	1	1	2	2	2	2	2	2	2	2	2	1	1.8

APPENDIX B:

Calculations

FIGURE 9.*

FIGURE 10.*

Area of Sector; A_s

$$A_s = \frac{\theta r^2}{2}$$

GIVEN:

$$\ell = 2\sqrt{2hr - h^2} \quad (approximate\ formula)$$

FROM   FIGURE 9.*: $Cos\ \theta/2 = \left(\dfrac{r-h}{r}\right) \longrightarrow \theta = 2\,Cos^{-1}\left(\dfrac{r-h}{r}\right)$
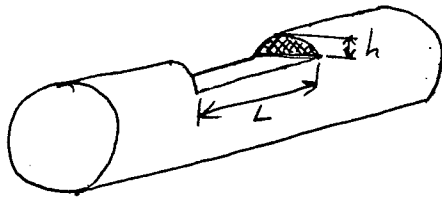
Now $AREA_{PCQ} = A_s - Area_{\angle OPQ}$

$$Area_{\angle OPQ} = 2\left(Area_{\angle OEQ}\right) = 2\left(\frac{1}{2}\frac{\ell}{2}(r-h)\right) = \frac{\ell}{2}(r-h)$$

So $AREA_{PCQ} = \dfrac{\theta r^2}{2} - \dfrac{\ell}{2}(r-h)$

and substituting for θ and ℓ;

$$Area_{PCQ} = r^2 Cos^{-1}\left(\frac{r-h}{r}\right) - (r-h)\sqrt{2hr - h^2}$$

TO FIND THE ABRASION VOLUME (VOLUME OF ABRADED MATERIAL)
AT EACH ABRASION LOCATION ON EACH CABLE:

where L = the length of the abrasion area, parallel to the
cable's longitudinal axis
h = wear depth, v = volume

Volume = AREA × length

$\therefore \quad v = L\left[r^2 \cos^{-1}\left(\frac{r-h}{r}\right) - (r-h)\sqrt{2hr - h^2} \right]$

NOTE THAT TO FIND THE TOTAL VOLUME, V, of the
ABRADED MATERIAL FROM ALL ABRASION LOCATIONS ON THE
RAFT OF CABLE SPECIMENS; THEN v MUST BE
CALCULATED for each location, then summed to
reach the TOTAL VOLUME V.

$$V = \sum_{i=1}^{12} \left[L_i \left[r^2 \cos^{-1}\left(\frac{r-h_i}{r}\right) - (r-h_i)\sqrt{2h_i r - h_i^2} \right]\right]$$